# ChemMedChem

## Accepted Article

**Authors:** Rati Kailash Prasad Tripathi, Ashish Dhirubhai Patel, Thopallada Yunus Pasha, Paras Lunagaria, Umang Shah, and Tushar Bhambharoliya

# A Library of Thiazolidin-4-one Derivatives as Protein Tyrosine Phosphatase 1B (PTP1B) Inhibitors: An Attempt to Discover Novel Anti-diabetic Agents

Dr. Ashish D. Patel,[b, c] Dr. Thopallada Y. Pasha,[d] Paras Lunagariya,[e] Dr. Umang Shah,[b] Tushar Bhambharoliya,[f] and Dr. Rati K. P. Tripathi*[a, c]

[a]     Dr. Rati K. P. Tripathi (Corresponding Author)*
        Department of Pharmaceutical Science, Sushruta School of Medical and Paramedical Sciences
        Assam University (A Central University), Silchar
        Assam 788011, India
        E-mail: rati.tripathi.phe09@iitbhu.ac.in
[b]     Dr. Ashish D. Patel, Dr. Umang Shah
        Ramanbhai Patel College of Pharmacy
        Charotar University of Science and Technology, Changa
        Anand 388421, India
[c]     Dr. Rati K. P. Tripathi, Dr. Ashish D. Patel
        Department of Pharmaceutical Chemistry
        Parul Institute of Pharmacy, Parul University, Vadodara
        Gujarat 391760, India
[d]     Dr. Thopallada Y. Pasha
        Shri Adichunchanagiri College of Pharmacy
        Adichunchanagiri University, B G Nagara
        Karnataka 571448, India
[e]     Paras Lunagariya
        Smt. R. D. Gardi B. Pharmacy College, Rajkot
        Gujarat 360110, India
[f]     Tushar Bhambharoliya
        Wilson College of Textiles
        North Carolina State University
        North Carolina 27606, United States

**Abstract:** Protein tyrosine phosphatase 1B (PTP1B) is an important target for treatment of diabetes. A series of thiazolidin-4-one derivatives **8-22** was designed, synthesized and investigated as PTP1B inhibitors. New molecules inhibited PTP1B with $IC_{50}$ in micromolar ranges. 5-(Furan-2-ylmethylene)-2-(4-nitrophenylimino)thiazolidin-4-one (**17**) exhibited maximum potency with competitive type of enzyme inhibition. SAR studies revealed various structural facets substantial for potency of these analogues. The findings revealed requirement of nitro group including hydrophobic heteroaryl ring for PTP1B inhibition. Molecular docking studies afforded good correlation between experimental and computational results. H-bonding and π–π interactions were responsible for optimal binding and effective stabilization of virtual protein-ligand complexes. Furthermore, *in-silico* pharmacokinetic properties of test compounds predicted their drug-like characteristics for potential oral use as anti-diabetic agents. Additionally, a binding site model demonstrating crucial pharmacophoric characteristics influencing potency and binding affinity of inhibitors has been proposed, which can be employed in the design of future potential PTP1B inhibitors.

## Introduction

Diabetes mellitus is one of the major global and continuously springing up public health burden discerned by raised plasma glucose level or hyperglycemias which has affected not only the adult populations but also the children.[1,2] According to International Diabetes Federation (IDF), in 2019, approximately 463 million adults (9.3% of total population) over 18 years of age and 136 million people above 65 years of age were reported to suffer from diabetes. The global health expenditure spent on diabetes was estimated to be USD 760 billion in 2019. Further, the global diabetes prevalence has been forecasted to rise from 9.3% (in 2019) to 10.2% (578 million) by 2030 and 10.9% (700 million) by 2045. The prevalence has been found to be higher in urban (10.8%) than rural (7.2%) areas, and in high-income (10.4%) than low-income countries (4.0%).[3] WHO projects that diabetes will be the seventh leading cause of death in 2030, with almost half of all the deaths attributable to high blood glucose.[4] It is categorized into two types *viz.* type I, also called juvenile diabetes or insulin-dependent diabetes mellitus (IDDM), and type II, also known as adult-onset diabetes or non-insulin-

dependent diabetes mellitus (NIDDM/T2DM).[5,6] Amongst these, type II diabetes is the most common type, comprising of >90% of reported cases, whereby the patients experience resistance towards insulin causing loss of glucose homeostasis. Insulin activates several intracellular signalling pathways that regulate cellular growth and metabolism.[6,7] Thus, T2DM is characterized by defects in signalling by the insulin receptor (IR) protein tyrosine kinase.[6] The currently existing therapies are restrained in that they demonstrate a number of adverse effects (for example, weight gain, headache, gastrointestinal complaints, hypotension, peripheral oedema, heartburn, anorexia, increased appetite, etc.), are costly and frequently ineffectual in producing an intended effect due to resistance.[8-10] Hence, the present scenario demands the discovery of novel therapeutic molecules to surmount this problem.[10,11]

In most of the multicellular organisms, a number of signaling cascades plays a very important role in the transmission of information in several biological processes. Among the several cascades, protein phosphorylation and dephosphorylation constitute one of the important post-translational modification mechanisms utilized by the cells regulate diverse cellular processes like growth, differentiation, metabolism, cell cycle, cell-cell communications, cell migration, gene transcription, ion channels, the immune response, survival, apoptosis, etc.[12-14] Tyrosine phosphorylation plays a crucial role in controlling various cellular and extracellular responses such as antigen-receptor signalling in B cells, T-cell activation, and gene expression. Any abnormality in these responses may result in a number of human diseases including diabetes, hypertension, cancer, rheumatoid arthritis, and others.[15-16] *In-vivo*, tyrosine phosphorylation is a reversible and dynamic process and is controlled by the counter-balancing activities of two enzymes *viz.* protein tyrosine kinases (PTKs) that catalyze phosphate transfer and protein tyrosine phosphatases (PTPs) that are responsible for phosphate hydrolysis.[17-19] The addition or removal of a phosphoryl moiety from a protein can engender a recognition motif for protein-protein interactions, control stability of protein, and significantly modulate enzymatic activity.[14,20,21]

Protein tyrosine phosphatases (PTPs) are a family of enzymes catalyzing the dephosphorylation of the tyrosine (Tyr)-phosphorylated proteins. They are responsible for exerting both positive and negative effects on a signalling pathway and play crucial physiological roles in various mammalian tissues and cells.[22-25] PTPs are characterized by the presence of the active site signature motif (H/V)C(X)$_5$R(S/T) in the conserved catalytic domain.[26-29] In addition to the catalytic domain, PTPs are embellished with a broad range of structural elements including SH2 domains, PDZ domains, extracellular ligand binding domains and many others.[30-32] Deregulation of PTP activity can contribute to the pathogenesis of many human diseases including diabetes.[33-35] Recently, studies on human genomic sequence reckoned that humans possess 112 PTPs, which include both the tyrosine-specific and dual-specific phosphatases. The tyrosine-specific phosphatases includes cytosolic non-receptor forms like PTP1B, SHP-1, SHP-2 that hydrolyze phosphotyrosine (pTyr)-containing proteins; and receptor-like transmembrane forms like CD45, RPTPµ, RPTPα;[36] while the dual-specific phosphatases includes CDC25, kinase-associated phosphatase and MAP kinase phosphatase-1 that utilize protein substrates containing pTyr, as well as phosphoserine (pSer) and phosphothreonine (pThr).[37-39]

Tyrosine-protein phosphatase non-receptor type 1, also known as protein-tyrosine phosphatase 1B [PTP1B, E.C. 3.1.3.48] belongs to tyrosine phosphatase (PTP) family of enzymes and is encoded by PTPN1 gene.[30,39,40] In insulin signaling pathway, both the insulin receptor β (IRβ) and insulin receptor substrate 1 (IRS-1) are substrates of PTP1B.[41] The insulin pathway is activated when insulin binds to their receptor, and auto-phosphorylation and activation takes place. The activated insulin receptor promotes tyrosine phosphorylation of insulin receptor substrate-1 (IRS-1), resulting in phosphatidyl-inositol-3-kinase (PI3K) and AKT activation including downstream lipid and glucose metabolism.[42-43] In the contrasting manner, PTP1B dephosphorylates the IRβ and IRS-1, and by that means, attenuates the insulin signaling pathway.[44] Studies on PTP1B knockout mice revealed that the PTP1B is a major negative regulator of insulin signaling in muscle and liver, and the loss of PTP1B activity leads to enhanced insulin sensitivity and resistance to weight gain in mice.[45-50] The findings suggested the possibility of treating type II diabetes and/or obesity with inhibitors that block PTP1B activity.[51-53] Thus, selective PTP1B inhibitors could potentially ameliorate insulin resistance and normalize plasma glucose and insulin without inducing hypoglycaemia. As a result, PTP1Bs represent novel molecular targets for the exploitation of medicaments possessing anti-diabetic or anti-obesity action.[52] However, the clinical translation of these PTP1B inhibitors has not been successful owing to lack of cell permeability and bioavailability. This is primarily because the catalytic site of PTP1B is positively charged at normal body pH and competitive inhibitors of PTP1B requires incorporation of a negatively charged pTyr mimetic group in their molecular framework for inhibitory potency.[54,55]

2

However, this negative charge reduces cell permeability and bioavailability which impedes clinical development.[56] Thus, small molecule PTP1B inhibitors with good enzyme binding affinity and devoid of any charged functional groups are highly desirable to combat the type II diabetes.

Small molecule inhibitors of this enzyme have been pursued in spatial extent both by industry and academia.[52,57-64] Although, there are no PTP1B inhibitors currently in the market; in the recent years, several PTP1B inhibitor drug candidates have reached clinical trials and are under development for the treatment of T2DM *viz.* trodusquemine also called MSI-1436 (NCT00509132, NCT00606112, NCT00806339), ISIS 113715 (NCT00327626, NCT00330200, NCT00330330, NCT00365781, NCT00455598), ISIS-PTP1BRx (NCT01918865), and Ertiprotafib (stopped after Phase II testing due to toxicity concerns), and JTT-551.[65-67] Additionally, a number of PTP1B inhibitors possessing different scaffolds, *viz.* benzooxathiazole derivatives, hydroxyphenylazole derivatives, piperazine derivatives, isothiazolidinone derivatives, thiazolidine-2,4-dione derivatives, 2-thioxothiazolidin-4-one derivatives, thiazolidinone derivatives, thiazolyl derivatives, and urea derivatives demonstrating high PTP1B binding affinity has been reported, but none of these has been found to show better cellular potency.[60,61,68-79] Examples of some thiazolidine and isothiazolidine derived compounds showing inhibition against PTP1B are illustrated in Figure 1 (compounds **1-4**).[60-64] Nevertheless, compounds possessing good potency and are promptly available to target tissues still remain elusive.[80,81]
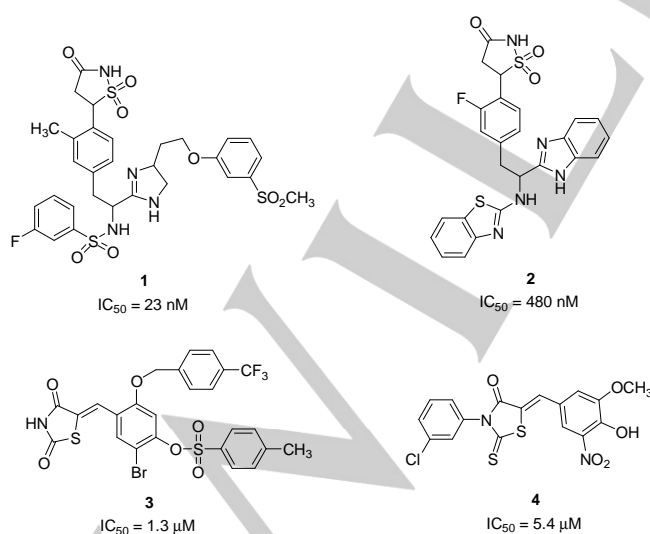


**Figure 1.** Structures of some potential PTP1B inhibitors bearing thiazolidine or isothiazolidine scaffold (compounds 1-4).[60-64]

Even though substantial advancements has been attained in the design of selective PTP1B inhibitors in the past decennia, a veritable breakthrough in the field happened only with the resolution of the three dimensional X-ray crystal structure of human PTP1B. More recently, the X-ray crystallographic structure of PTP1B complexed with several inhibitors has been reported.[82,83] These developments have made possible a more detailed understanding of the binding between PTP1B inhibitors and the protein as well as in deciphering the mechanisms of action and inhibition of PTP1B. As a result, computational simulations coupled with structure – activity relationship studies may now be used to mimic interactions within the active site of the enzyme and to understand the insidious factors that govern PTP1B inhibitory activity and selectivity.

Espousing an initial study on PTP1B inhibitors, we have reported the synthesis, *in-silico* and PTP1B inhibitory activity of novel 1,6-dihydropyrimidine derivatives, some of which proved to be potent PTP1B inhibitors.[84] In line of the above mentioned conceptions and retaining all the pertinent structural variants on PTP1B, the objective of the present study is to design and synthesize a library of compounds that constitute the thiazolidin-4-one scaffold linked to either thiophene, furan or imidazole moiety *via* methylene linkage on one side and connected to various aromatic nuclei through imino linkage on the other side (Figure 2 and Scheme 1) and investigate their PTP1B inhibitory activity. The designing strategy for the proposed compounds has been illustrated in Figure 2. The compounds were designed employing CADD approaches and following the 3D-QSAR model proposed by Saxena and co-workers for PTP1B inhibitors taking into consideration the essential structural features influencing the PTP1B activity.[85,86] The substitution pattern of the designed molecules was deliberately chosen on compound **I** in such a way as to bestow them different lipophilic and electronic properties to dig into the detailed structure-activity relationship (SAR) for *in-vitro* PTP1B inhibition.[76] Additionally, to understand the reason for observed PTP1B inhibitory activity, molecular docking simulations as well as conformational alignment studies were performed in order to rationalize and correlate the obtained biological results and to get more insight into the various interactions between the ligands and enzyme active sites in detail. These modeling studies were performed using cheminformatic tools like ChemDraw Professional 15.0, Chem3D 15.0, ChemAxon Tools, AutoDock 4.2, and Discovery Studio 3.1.[87,88] These data are accompanied by an *in-silico* evaluation of molecular property and pharmacokinetic properties using online prediction platforms like pkCSM and ProTox, with

3

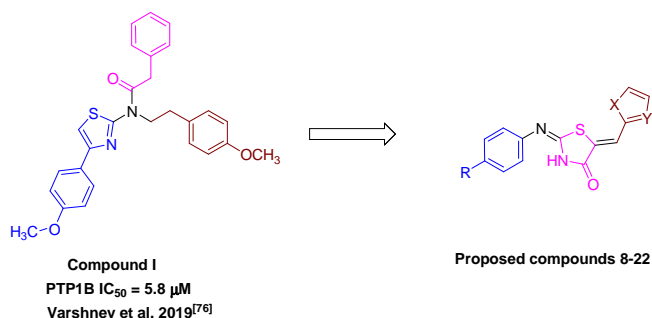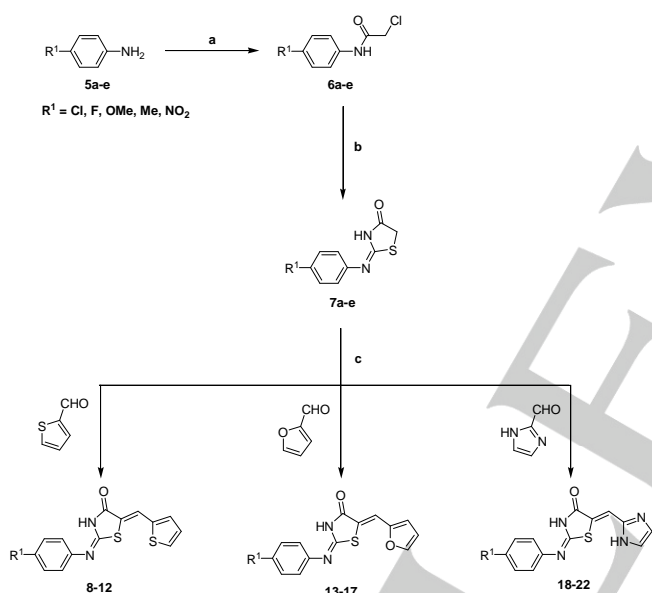the goal of earning prelude info pertaining to their drug-like profile.[89-91]



**Compound I**
**PTP1B IC$_{50}$ = 5.8 µM**
**Varshney et al. 2019[76]**

**Proposed compounds 8-22**

**Figure 2.** Designing strategy for proposed compounds **8**-**22**.

## Results and Discussion

### Chemistry



**Scheme 1.** Reagents and conditions: **a.** ClCH$_2$COCl, Dry THF, reflux, 7-8 h; **b.** NH$_4$SCN, EtOH, reflux, 4-5 h; **c.** EtOH, reflux, 80$^0$C, 10-12 h.

Fifteen new thiazolidin-4-one derivatives **8-22** presented in this work were synthesized using a well-established synthetic route depicted in Scheme 1 following the standard reaction conditions.[92,93] The first intermediates 2-chloro-N-(4-aryl-substituted phenyl)acetamides **6a-e** were synthesized in quantitative amount from the commercially available 4-substituted anilines **5a-e** on reaction with chloroacetyl chloride. The corresponding 2-(4-aryl-substituted phenyl)iminothiazolidine-4-ones **7a-e** was efficiently prepared by the reaction of **6a-e** with ammonium thiocyanate. Finally, the target products **8-22** were obtained by the reaction of

compounds **7a-e** (0.0022 mol) with appropriate thiophene-2-carbaldehyde, furan-2-carbaldehyde and *1H*-imidazole-2-carbaldehyde (Scheme 1). The physicochemical and spectral characterization data of all the synthesized compounds were in good agreement with their structures and are demonstrated in Experimental Section. Elemental analysis showed C, H and N within ± 0.4% of the calculated values. The physicochemical characterization data for the final compounds **8-22** are presented in Table 1.

**Table 1.** Physicochemical characterization data of final compounds **8-22**.



| Compd | R$^1$ | M.P. (°C) | Yield (%) | cLogP[a] | R$_f$[b] |
|-------|-------|-----------|-----------|----------|----------|
| **8** | Cl | 236-238 | 48 | 2.55 | 0.56 |
| **9** | F | 231-233 | 58 | 1.98 | 0.52 |
| **10** | OMe | 226-228 | 61 | 1.76 | 0.61 |
| **11** | Me | 211-213 | 56 | 2.34 | 0.71 |
| **12** | NO$_2$ | 246-248 | 40 | 1.58 | 0.42 |
| **13** | Cl | 213-215 | 65 | 2.08 | 0.51 |
| **14** | F | 205-207 | 50 | 1.51 | 0.48 |
| **15** | OMe | 229-231 | 62 | 1.29 | 0.63 |
| **16** | Me | 234-236 | 66 | 1.87 | 0.70 |
| **17** | NO$_2$ | 239-241 | 45 | 1.11 | 0.45 |
| **18** | Cl | 233-235 | 55 | 0.74 | 0.64 |
| **19** | F | 236-238 | 49 | 0.17 | 0.54 |
| **20** | OMe | 242-244 | 45 | -0.05 | 0.68 |
| **21** | Me | 238-240 | 52 | 0.52 | 0.72 |
| **22** | NO$_2$ | 256-258 | 58 | -0.23 | 0.42 |

[a] MarvinSketch 5.6 generated. [b] Solvent system – CHCl$_3$:CH$_3$OH (9:1).

### *In-vitro* PTP1B inhibition assay

To better understand the structural prerequisites for inhibitory activity of PTP1B, the final compounds **8-22** were evaluated for inhibition potential towards PTP1B *in-vitro* using Calbiochem PTP1B colorimetric assay kit using suramin as reference.[94] The inhibitory activities were examined by measuring the effects of each compound on the production of free phosphate from IR5 phosphopeptide substrate and the results of inhibition assay is

4

expressed in terms of IC$_{50}$ values and are summarized in Table 2.

**Table 2.** *In-vitro* and computational PTP1B inhibition data for compounds **8-22**.

| Compd | *In-vitro* | Computational | |
|---|---|---|---|
| | IC$_{50}$ (µM) ± SEM | ΔG (kcal mol$^{-1}$) | K$_i$ (µM) |
| **8** | 19.98 ± 0.14 | -5.8 | 56.08 |
| **9** | 26.87 ± 0.18 | -5.3 | 129.97 |
| **10** | 17.45 ± 0.11 | -5.37 | 114.95 |
| **11** | 9.79 ± 0.15 | -5.96 | 43.07 |
| **12** | 6.42 ± 0.08 | -8.41 | 0.689 |
| **13** | 9.17 ± 0.13 | -6.02 | 38.85 |
| **14** | 21.96 ± 0.17 | -5.77 | 58.81 |
| **15** | 12.20 ± 0.08 | -5.57 | 82.65 |
| **16** | 8.45 ± 0.09 | -6.35 | 22.07 |
| **17** | 5.88 ± 0.06 | -8.05 | 1.26 |
| **18** | 29.78 ± 0.09 | -5.28 | 134.13 |
| **19** | 14.24 ± 0.06 | -6.0 | 40.25 |
| **20** | 13.02 ± 0.07 | -5.53 | 87.97 |
| **21** | 11.14 ± 0.16 | -5.53 | 88.44 |
| **22** | 7.93 ± 0.12 | -7.41 | 3.68 |
| **Suramin** | 10.98 ± 1.13 | - | - |
| **BTC** | 210 nM[a] | -9.98 | 0.048 |

**NOTE:** Each IC$_{50}$ value is the mean ± SEM. It refers to the assay concentration of test compound which leads to 50% inhibition of enzyme activity. Level of statistical significance: $P < 0.05$ versus the corresponding IC$_{50}$ values obtained against PTP1B, as determined by ANOVA/Dunnett's. Reference inhibitors: Suramin, BTC: 4-Bromo-3-(carboxymethoxy)-5-[3-(cyclohexylamino)phenyl]thiophene-2-carboxylic acid. [a] – Data expressed in terms of K$_i$.

In general, the synthesized compounds displayed good to moderate activity profiles in the PTP1B inhibition assay, with IC$_{50}$ values ranging from 5.88 ± 0.06 µM (compound **17**) to 29.78 ± 0.09 µM (compound **18**). Modifications in the steric and electronic characteristics of the test compounds (**8-22**) afforded by the introduction of various mono-substitutions (*viz.* Cl, F, OCH$_3$, CH$_3$, and NO$_2$) at *para*-position on the phenyl ring attached to iminothiazolidine-4-one scaffold on one side and 5-membered heteroaromatic ring on the other side (*viz.* thiophene, furan, imidazole ring) of the scaffold significantly influenced the inhibitory profile of these compounds. Interestingly, compounds possessing furan ring (**13-17**) showed better PTP1B inhibition followed by those with thiophene (**8-12**) and imidazole (**18-22**) rings. 5-(Furan-2-ylmethylene)-2-(4-nitrophenylimino)thiazolidin-4-one (**17**) was found to be the most promising PTP1B inhibitor amongst other compounds with IC$_{50}$ value of 5.88 ± 0.06 µM. The second best inhibition profile was observed for 2-(4-nitrophenylimino)-5-(thiophen-2-ylmethylene)thiazolidin-4-one (**12**) displaying an IC$_{50}$ of 6.42 ± 0.08 µM, followed by 5-((1H-imidazol-2-yl)methylene)-2-(4-nitrophenylimino)thiazolidin-4-one (**22**) with IC$_{50}$ of 7.93 ± 0.12 µM respectively. Surprisingly, all these inhibitors (compounds **17**, **12**, and **22**) possessed –NO$_2$ group at *para*-position of the phenyl ring thus indicating that –NO$_2$ group seemed to play an important role for PTP1B inhibition. Similar observations pointing out to the fact that the presence of the –NO$_2$ group exhibited a pronounced enhancement in the PTP1B inhibitory activity has been evidenced in various literatures published earlier by Saxena and group, which further strengthened our findings claiming the crucial role of the –NO$_2$ group for potent PTP1B inhibition.[70,78,79,86] Further, compounds bearing 4-CH$_3$ (compounds **11**, **16**, and **21**) and 4-OCH$_3$ (compounds **15**, **20**, **10**) substitutions on phenyl ring showed moderate inhibition against PTP1B, however, less than compounds possessing 4-NO$_2$ group (compounds **17**, **12**, and **22**). Presence of electron-withdrawing –Cl or –F groups further reduced the activity with some exceptions (compound **13**).

**Kinetic measurements of lead PTP1B inhibitor 17**



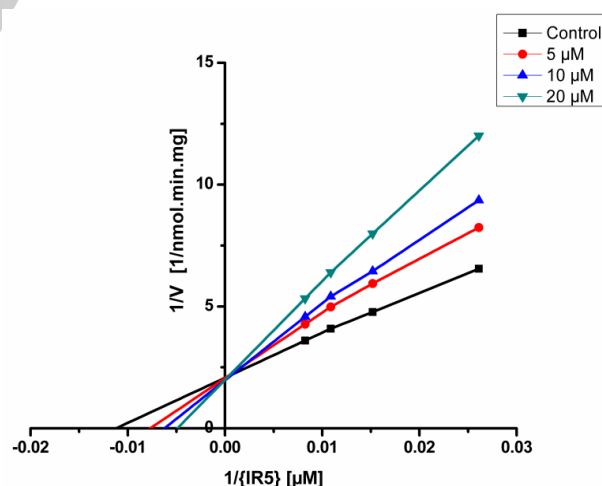**Figure 3.** Kinetics of human recombinant PTP1B inhibition by compound **17** in the absence (control) and presence of various concentrations of compound **17** (5 µM, 10 µM, 20 µM) with varying concentration of substrate IR5. Rate data are expressed as nmol product formed/min/mg enzyme.

A kinetic study was carried out with inhibitor **17**, the selected representative lead PTP1B inhibitor, to ascertain the inhibition

5

mechanism of these compounds against human recombinant PTP1B, expressed on *E.coli*. The type of inhibition was established from the analysis of Lineweaver-Burk reciprocal plots, which demonstrated that the lines intersected at the Y-axis with increase in the $K_m$ values and constant $V_{max}$ suggesting a competitive type of PTP1B inhibition pattern (Figure 3).

### Determination of $K_i$

To acquire information with regards to the strength of interactions between inhibitor and the enzyme, the dissociation constant ($K_i$) was computed for the inhibitor for each inhibition mode. $K_i$ value for competitive inhibitor **17** was calculated using the GraphPad Prism software (version 5.0) and was found to be 16.98 ± 2.69 μM.

### Molecular modeling simulations

The experimental *in-vitro* results of PTP1B inhibitory activity is further supported by molecular docking studies using AutoDock 4.2. The studies were carried out to ascertain the binding orientation and characterize the essential structural requirements for key interactions of the tested compounds (**8-22**) and residues involved in the binding within the active site of PTP1B enzyme using the X-ray crystal structure of PTP1B (PDB ID: 2QBS) retrieved from Protein Data Bank. Docking was performed following the protocol presented in literature.[95] Iterative gold standard pose (GSP) analysis was carried out for the cross-validation of docking poses, for which troubleshooting was accomplished to eliminate problematic structures. The results are expressed in terms of predicted binding free energies (ΔG, kcal mol$^{-1}$) and theoretical inhibition constants ($K_i$, μM) for each virtual PTP1B-inhibitior complex and illustrated in Table 2. The computational results were found to be in good correlation with the experimental data, thus corroborating our hypothesis.

### Pose analysis of PTP1B inhibitors

Visual examination of the computationally docked optimal binding poses of all the inhibitors within the active site of PTP1B enzyme revealed that the ligands occupied the catalytic loop of PTP1B binding pocket comprising of PTP signature motif lined by the residues His214, Cys215, Ser216, Ala217, Gly218, Ile219, Gly220, and Arg221; the WPD loop formed by the residues Asp181, Arg221, and Gln262; and the YRD motif surrounded by Tyr46, Arg47, and Asp48 (Figure 4). Furthermore, the key factors that stabilized the ligand-enzyme complex included various types of interactions *viz.* hydrogen bonding and

hydrophobic interactions, playing a very important role in binding, including π – π stacking, π – cation, and π – σ interactions as well.
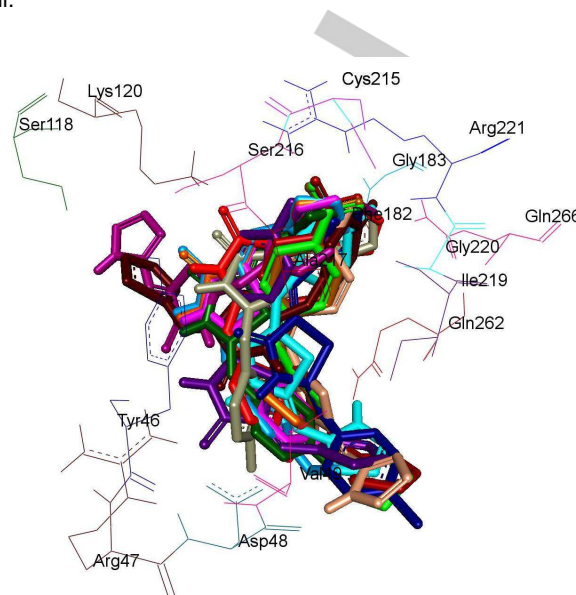


**Figure 4.** Structural screenshot of superimposed PTP1B inhibitors docked into the PTP1B active site. Selected amino acid residues are depicted in black. Shared binding modes of compounds **8-22** are displayed in dark blue, dark brown, dark violet, dark green, maroon, pink, orange, sky blue, grey, fluorescent green, light orange, red, magenta, fluorescent blue, and light brown, respectively.

All compounds showed one or more hydrogen bonding interactions except compound **8**. It was found that Arg24, Tyr46, Asp48, Lys120, Phe182, Cys215, Ser216, Ala217, Arg221, Gln262, and Gln266 were the major amino acids involved in hydrogen bonding with the test compounds. Hydrogen bonding interactions with residue Arg24 was observed for compound **17**, likewise with Tyr46 for compounds **9**, **14-16**, and **19**; with Asp48 for compounds **18** and **22**; with Lys120 for compounds **16** and **19**; with Phe182 for compounds **9** and **16**; with Cys215 for compounds **12**, **17**, and **22**; with Ser216 for compounds **12**, **14**, **15**, **17**, and **22**; with Ala217 for compounds **11**, **13**, and **14**; with Arg221 for compounds **10**, **12-20**, and **22**; with Gln262 for compounds **17**, **18**, and **21**; and with Gln266 for compound **9**. In addition, all the compounds exhibited hydrophobic (π – π stacking, π – cation, and π – σ) interactions with Arg24, Tyr46, Arg47, Lys120, Phe182, Ala217, Gly220, and Arg221; except **17** and **22** which did not show any π – π interactions. π – π interactions has been observed between residue Tyr46 and compounds **9**, **10**, and **20**; and Phe182 and compounds **8**, **16**, and **19**. Besides, π – cation interactions has been found between residue Arg24 and compounds **12**, **18**, and **21**; likewise between Arg47 and compounds **11**, **14**, **15**, and **16**; between Lys120 and compounds **9** and **21**; and between Arg221 and

6

compounds **8**, **11**, **13**, **14**, and **15**. Additionally, compound **9** was stabilized by a π – σ interaction with Lys120, compounds **12** and **19** by similar interactions respectively with Ala217 and Gly220. These docking results were found to be in congruence with that reported in previous studies by other researchers, thereby corroborating our findings.[70,76,78,79,86]

**Binding mode of lead PTP1B inhibitor 17**

Inspection of the best-ranked virtual complex of PTP1B and lead inhibitor **17** demonstrated compound **17** (ΔG = -8.05 kcal mol$^{-1}$; $K_i$ = 1.26 μM) to be located within the catalytic binding pocket comprising of PTP signature motif, WPD loop and YRD motif (Figure 5 (A)). The molecule has been found to be stabilized by various hydrogen bonding interactions, *viz.* between oxygen of furan ring and HH21 of Arg24 (interplanar distance of ~2.07 Å);

between oxygen of C=O of thiazolidin-2-one and HE21 of Gln262 (interplanar distance of ~2.24 Å); between the both the oxygen atoms of nitro group and SG of Cys215 (interplanar distance of ~3.18 Å and ~3.10 Å), H of NH of Ser 216 (interplanar distance of ~2.06 Å), HH21, HE and HN of Arg221 (interplanar distances of 2.02 Å, 2.2 Å and 1.78 Å) (Figure 5 (B) and (C)). No π – π interactions has been observed in PTP1B:**17** complex (Figure 5 (B) and (C)) thereby suggesting that the greater activity of the molecule may be attributed to higher number of hydrogen bonding interactions occurring between the enzyme-inhibitor complex. Superimposition of the PTP1B:**17** complex with the PTP1B-BTC complex suggested that compound **17** mimics the binding mode of the GSP (gold standard pose) ligand (BTC, 4-bromo-3-(carboxymethoxy)-5-[3-(cyclohexylamino)phenyl]thiophene-2-carboxylic acid) (Figure 5 (D)).
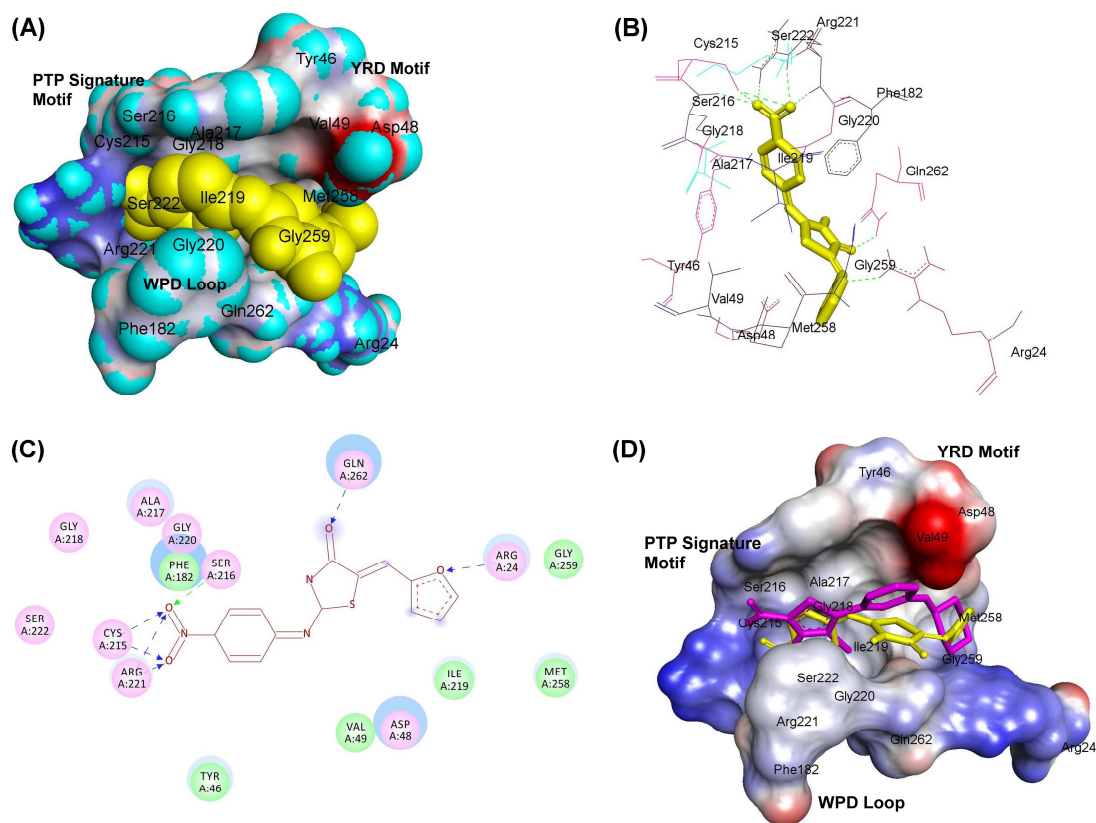


**Figure 5.** (A) Volume representation of **17** (yellow) in the PTP1B active site comprising of PTP signature motif, WPD loop and YRD motif (PDB ID:2QBS). (B) Best-ranked 3D molecular docking pose for virtual PTP1B – **17** complex showing hydrogen bonding (green dashed lines) interactions. (C) The 2D representation of the binding interactions of compound **17** (maroon) within PTP1B active site. The arrows represent hydrogen bonding. (D) Superimposed binding mode of compound **17** (yellow), originally docked with GSP ligand BTC (4-bromo-3-(carboxymethoxy)-5-[3-(cyclohexylamino)phenyl]thiophene-2-carboxylic acid; pink; PDB ID:2QBS).

**Comparison of experimental and computational results**

The ranking order of inhibitors **8-22** for potency against PTP1B as per the experimental and computational data is presented in

7

Table 3. These data indicated almost a good to better correlation between the experimental (*in-vitro*) and computational data for PTP1B inhibition, thus supporting our hypothesis.

**Table 3.** Comparison of experimental and computational activity data for compounds **8-22**.

| Activity | Experimental results (IC$_{50}$ value) | Computational results (ΔG value) |
|---|---|---|
| PTP1B | 17 > 12 > 22 > 16 > 13 > 11 > 21 > 15 > 20 > 19 > 10 > 8 > 14 > 9 > 18 | 12 > 17 > 22 > 16 > 13 > 19 > 11 > 8 > 14 > 15 > 20 > 21 > 10 > 9 > 18 |

**In-silico drug-likeness and pharmacokinetic property prediction**

All the structural elements were selected to adhere to values of Lipinski's rules for possible drug-likeness using pkCSM server

(Table 4). The lipophilicity (expressed as LogP) predicted for all the compounds were found to be well the traditionally cut-off value of 5 used in drug design. All the structures reported herein show suitable MW values (MW < 500) necessary for a successful penetration through biological membranes. The surface area (SA) for all the compounds was observed to be in the range 117.58-133.27 Å$^2$ which is well within the limit. Thus, the predicted values for all compounds **8-22** fall into the appropriate range indicating good bioavailability of the candidate molecule. The number of hydrogen bond acceptors (HBA, ≤10) and donors (HBD, ≤5) for all the compounds were in accordance with the Lipinski's rule of five. Thus it was predicted that all compounds are likely to be orally active.

**Table 4.** *In-silico* prediction of drug-likeness for title compounds **8-22**[a].

| Compd | MW | LogP | SA | HBA | HBD | n$_{violations}$ | Rotatable bonds |
|---|---|---|---|---|---|---|---|
| **8** | 320.83 | 4.29 | 128.93 | 4 | 1 | 0 | 2 |
| **9** | 304.37 | 3.78 | 122.79 | 4 | 1 | 0 | 2 |
| **10** | 316.41 | 3.65 | 130.10 | 5 | 1 | 0 | 3 |
| **11** | 300.41 | 3.95 | 124.98 | 4 | 1 | 0 | 2 |
| **12** | 331.38 | 3.55 | 133.27 | 6 | 1 | 0 | 3 |
| **13** | 304.76 | 3.83 | 124.08 | 4 | 1 | 0 | 2 |
| **14** | 288.30 | 3.31 | 117.94 | 4 | 1 | 0 | 2 |
| **15** | 300.34 | 3.18 | 125.26 | 5 | 1 | 0 | 3 |
| **16** | 284.34 | 3.48 | 120.14 | 4 | 1 | 0 | 2 |
| **17** | 315.31 | 3.07 | 128.43 | 6 | 1 | 0 | 3 |
| **18** | 304.76 | 2.96 | 123.72 | 4 | 2 | 0 | 2 |
| **19** | 288.31 | 2.44 | 117.58 | 4 | 2 | 0 | 2 |
| **20** | 300.34 | 2.31 | 124.89 | 5 | 2 | 0 | 3 |
| **21** | 284.34 | 2.61 | 119.78 | 4 | 2 | 0 | 2 |
| **22** | 315.31 | 2.21 | 128.06 | 6 | 2 | 0 | 3 |

[a] MW = Molecular weight, LogP = octanol-water partition coefficient, SA = Surface Area, HBA = Number of hydrogen bond acceptor, HBD = Number of hydrogen bond donor, n$_{violations}$ = violations from Lipinski's rule

Additionally, a variety of key ADMET (Absorption, Distribution, Metabolism, Excretion and Toxicity) properties has also been calculated with the aid of servers, pkCSM and ProTox. The results are listed in Table 5 and Table 6 respectively. All compounds showed moderate to high water solubility ranging from -2.41 log mol/L (compound **21**) to -5.03 log mol/L

(compound **8**), in addition to high Caco-2 permeability (permeation > 0.90) except compound **12** (permeation = 0.77) which showed moderate and **22** (permeation = -0.16) which showed poor permeability. Intestinal absorption (IA) has been found to be greater than 85% indicating good permeation across the intestinal membrane. Further, compounds **10**, **12-15**, and **17-**

8

**22** showed good permeation through skin (permeation > -2.5) while compounds **8**, **9**, **11**, and **16** showed poor skin permeability (permeation < -2.5). Additionally, all compounds showed no inhibition towards P-glycoprotein I and P-glycoprotein II, except compounds **8**, **9**, and **10** which demonstrated inhibition towards P-glycoprotein I. Furthermore, all compounds showed poor BBB permeability and moderate CNS permeability. None of the compounds showed inhibition towards the metabolizing enzyme CYP3A4, while compounds **8-**

**17** showed inhibition towards CYP2C9, indicating that these compounds can potentially stop the metabolism of xenobiotic agents. The compounds **8-22** were found to show the total clearance in the range -0.27 (log mL/min/kg) to 0.65 (log mL/min/kg). Futher, no compounds other than **9**, **10**, **17**, **21**, and **22** were found to act as OCT2 substrate, thus indicating the potential of these compounds for adverse interactions and their negative effect on renal clearance.

**Table 5.** *In-silico* ADME prediction for title compounds **8-22**[a].

| Compd | Absorption | | | | | | | Distribution | | | Metabolism | | Excretion | |
|---|---|---|---|---|---|---|---|---|---|---|---|---|---|---|
| | WS | CP | IA | SP | PI-1 | PI-2 | VD | FU | BBB | CNS | CI-1 | CI-2 | TC | RS |
| **8** | -5.03 | 1.64 | 89.42 | -2.31 | Yes | No | 0.28 | 0 | 0.10 | -1.63 | No | Yes | -0.26 | No |
| **9** | -4.79 | 1.58 | 90.37 | -2.42 | Yes | No | 0.09 | 0 | -0.02 | -1.66 | No | Yes | -0.27 | Yes |
| **10** | -4.81 | 1.39 | 91.87 | -2.55 | Yes | No | 0.15 | 0 | -0.14 | -1.96 | No | Yes | -0.09 | Yes |
| **11** | -4.67 | 1.79 | 90.60 | -2.25 | No | No | 0.33 | 0 | 0.16 | -1.62 | No | Yes | -0.18 | No |
| **12** | -4.61 | 0.77 | 88.36 | -2.62 | No | No | 0.25 | 0 | -0.73 | -2.01 | No | Yes | -0.11 | No |
| **13** | -4.37 | 1.41 | 91.24 | -2.55 | No | No | 0.05 | 0.14 | 0.08 | -1.79 | No | Yes | -0.11 | No |
| **14** | -4.01 | 1.37 | 92.19 | -2.83 | No | No | -0.12 | 0.17 | -0.05 | -1.96 | No | Yes | -0.13 | No |
| **15** | -4.05 | 0.96 | 93.69 | -2.99 | No | No | -0.05 | 0.16 | -0.17 | -2.81 | No | Yes | 0.05 | No |
| **16** | -3.81 | 1.40 | 92.42 | -2.49 | No | No | 0.09 | 0.12 | 0.13 | -1.83 | No | Yes | -0.04 | No |
| **17** | -3.96 | 0.96 | 95.18 | -2.63 | No | No | -0.02 | 0.02 | -0.75 | -2.13 | No | Yes | 0.03 | Yes |
| **18** | -2.58 | 0.98 | 85.03 | -2.74 | No | No | 0.55 | 0.35 | -0.94 | -2.11 | No | No | 0.62 | No |
| **19** | -2.51 | 0.97 | 86.04 | -2.75 | No | No | 0.41 | 0.39 | -0.92 | -2.27 | No | No | 0.58 | No |
| **20** | -2.53 | 0.99 | 87.53 | -2.75 | No | No | 0.4 | 0.39 | -0.91 | -2.95 | No | No | 0.65 | No |
| **21** | -2.41 | 0.89 | 86.25 | -2.75 | No | No | 0.58 | 0.31 | -0.76 | -2.15 | No | No | 0.63 | Yes |
| **22** | -2.63 | -0.16 | 86.31 | -2.74 | No | No | 0.64 | 0.15 | -0.96 | -2.45 | No | No | 0.36 | Yes |

Abbreviations: WS – Water solubility (log mol/L), CP – Caco2 permeability (log Papp in $10^{-6}$ cm/s), IA – Human intestinal absorption (% Absorbed), SP – Skin permeability (log Kp), PI-1 – P-glycoprotein I inhibitor, PI-2 – P-glycoprotein II inhibitor, VD – Human volume of distribution (log L/kg), FU – Fraction unbound (human) (Fu), BBB – BBB permeability (log BB), CNS – CNS permeability (log PS), CI-1 – CYP3A4 inhibitor, CI-2 – CYP2C9 inhibitor, TC – Total clearance (log mL/min/kg), RS – Renal OCT2 (organic cation transporter 2) substrate

With respect to toxicity (Table 6), compounds **8-11** and **14-15** showed negative response to the AMES test while compounds **12-13** and **16-22** showed positive response and hence can be predicted to be mutagenic. Maximum recommended tolerated dose (human) for the compounds under investigation were predicted to lie in the range of -0.22 log mg/kg/day (compound **17**) to 0.54 log mg/kg/day (compound **22**), thus indicating that all compounds except **22** showed low MRTD. Besides, the compounds **8-22** were predicted to be ineffective as hERG I (human ether-a-go-go gene I) inhibitors; however compounds **8**,

**11**, and **18-22** were predicted to be hERG II inhibitors indicating the potential of these compounds (**8**, **11**, and **18-22**) for the development of long QT syndrome – leading to fatal ventricular arrhythmia. Oral rat acute toxicity (ORAT) model predicted $LD_{50}$ (the amount of a compound given all at once that causes the death of 50% of a group of test animals) values to lie in the range of 2.32 mol/kg (compound **20**) to 2.93 mol/kg (compound **17**). Moreover, oral rat chronic toxicity (ORCT) model predicted the LOAEL (lowest dose of a compound that results in an observed adverse effect) values to lie in the range of 0.92 log mg/kg_bw/day (compound **13**) to 1.72 log mg/kg_bw/day

9

(compound **9**). No other compounds except **9-13**, and **15-16** were predicted to disrupt the normal functioning of the liver, demonstrating their hepatotoxic potential. None of the

compounds were predicted to be skin sensitive or cytotoxic. However, all the compounds were found to show *T.pyriformis* and minnow toxicity.

**Table 6.** *In-silico* toxicity prediction for title compounds **8-22**[a].

| Compd | AT | MRTD | hERGI | hERGII | ORAT | ORCT | HT | SS | TPT | MT | CT |
|---|---|---|---|---|---|---|---|---|---|---|---|
| **8** | No | 0.239 | No | Yes | 2.72 | 1.03 | No | No | 2.73 | -0.16 | No |
| **9** | No | 0.241 | No | No | 2.59 | 1.72 | Yes | No | 2.27 | 0.29 | No |
| **10** | No | 0.238 | No | No | 2.67 | 1.48 | Yes | No | 2.29 | 0.20 | No |
| **11** | No | 0.205 | No | Yes | 2.61 | 1.11 | Yes | No | 2.64 | 0.07 | No |
| **12** | Yes | -0.139 | No | No | 2.91 | 1.38 | Yes | No | 1.59 | -0.27 | No |
| **13** | Yes | 0.118 | No | No | 2.74 | 0.92 | Yes | No | 2.19 | 0.26 | No |
| **14** | No | 0.092 | No | No | 2.55 | 1.61 | No | No | 1.74 | 0.71 | No |
| **15** | No | 0.12 | No | No | 2.65 | 1.28 | Yes | No | 1.64 | 0.64 | No |
| **16** | Yes | -0.03 | No | No | 2.66 | 1.03 | Yes | No | 2.13 | 0.44 | No |
| **17** | Yes | -0.22 | No | No | 2.93 | 1.26 | No | No | 1.71 | 0.05 | No |
| **18** | Yes | 0.03 | No | Yes | 2.56 | 1.50 | No | No | 0.29 | 1.88 | No |
| **19** | Yes | -0.14 | No | Yes | 2.33 | 1.59 | No | No | 0.29 | 2.42 | No |
| **20** | Yes | -0.05 | No | Yes | 2.32 | 1.48 | No | No | 0.29 | 2.25 | No |
| **21** | Yes | 0.11 | No | Yes | 2.60 | 1.41 | No | No | 0.29 | 2.03 | No |
| **22** | Yes | 0.54 | No | Yes | 2.38 | 1.46 | No | No | 0.29 | 2.14 | No |

[a] AT – AMES toxicity, MRTD – Maximum recommended tolerated dose (human, log mg/kg/day), hERGI – hERG I inhibitor, hERGII – hERG II inhibitor, ORAT – Oral rat acute toxicity ($LD_{50}$, mol/kg), ORCT – Oral rat chronic toxicity (lowest dose of a compound that results in an observed adverse effect (LOAEL), log mg/kg_bw/day), HT – Hepatotoxicity, SS – Skin sensitization, TPT – *T.pyriformis* toxicity (log μg/L), MT – Minnow toxicity (log mM), CT – Cytotoxicity

To sum up, despite other compounds exhibiting good ADMET profiles, it can be concluded that compound **17** presents the best drug-like characteristics and ADMET properties among all the compounds of the series.

## Conclusion

Summarily, in the present work, a series of thiazolidin-4-one derivatives **8-22** have been investigated for PTP1B inhibition aimed at gathering information about their potential application as anti-diabetic agents. Interestingly, PTP1B inhibitory activities of these compounds revealed some highly potent PTP1B inhibitors. The most active compound 5-(Furan-2-ylmethylene)-2-(4-nitrophenylimino)thiazolidin-4-one (**17**) showed maximum PTP1B inhibition ($IC_{50}$ = 5.88 ± 0.06 μM). Further, kinetic studies revealed that compound **17** exhibited a competitive type of enzyme inhibition against PTP1B. SAR studies revealed various structural facets substantial for the potency of these analogues.

Particularly, our findings indicated the requirement of nitro group attached to aromatic ring including a hydrophobic heteroaryl moiety (furan or thiophene) for potential PTP1B inhibition. In addition, molecular docking simulations afforded a satisfactory correlation between the experimental and computational results and provided insight into the binding orientation and essential structural requirements for key interactions within the active site of PTP1B. The compounds were found to interact with the enzymes through H-bonding and hydrophobic (π – π, π – cation, and π – σ) interactions and were found to be responsible for optimal binding and effective stabilization of virtual protein-ligand complexes. Furthermore, *in-silico* pharmacokinetic properties of the test compounds predicted the drug-like characteristics for potential oral use as anti-diabetic agents. Thus, the better potency of compound **17** against PTP1B establishes it a potential candidate for advanced study in an attempt to develop novel anti-diabetic agents.

10

Based on the above study, a binding site model for PTP1B inhibitors demonstrating the crucial pharmacophoric characteristics influencing the potency and binding affinity of inhibitors is proposed (Figure 6), which can be employed in the design of future potential PTP1B inhibitors.
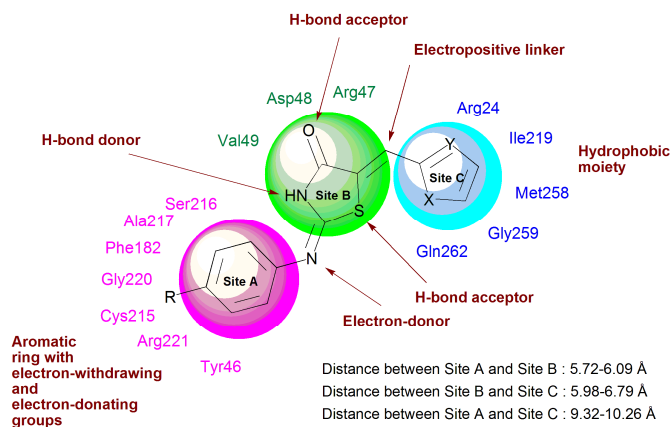


**Figure 6.** Proposed binding site model for PTP1B inhibitors showing essential pharmacophoric features

## Experimental Section

### Chemistry

Starting materials and reagents were procured from commercial suppliers Sigma-Aldrich and Merck and were used without further purification. The progress of the reactions was monitored using thin-layer chromatography (TLC) on silica gel pre-coated aluminum sheets (Type 60 F254; Merck; Germany). Melting points were determined by one end open capillaries on a VEEGO microprocessor based melting point apparatus using silicone oil bath and are uncorrected. IR spectra of intermediates and final compounds were recorded as potassium bromide pellets on BRUKER OPTICS ALPHA II FT-IR spectrometer. Dry solvents were used throughout. $^1$H and $^{13}$C NMR spectra were recorded on BRUKER AVANCE II 400 MHz FT-NMR spectrometer at the operating frequency of 400 MHz and 100 MHz respectively. Spectra were acquired using either CDCl$_3$ or DMSO-d$_6$ as solvent. Tetramethylsilane (TMS) was used as an internal reference. Chemical shifts (δ) for $^1$H and $^{13}$C NMR spectra were reported in parts per million (ppm) using the residual solvent line as the internal standard. Coupling constants (J) were expressed in Hertz (Hz). Multiplicities are recorded as s (singlet), d (doublet), t (triplet), dd (doublet of doublets), m (multiplet). The mass spectra were measured on a Thermo LCQ Advantage Max Ion Trap Mass spectrometer. Atmospheric pressure ionization electrospray (API-ES) mass spectra were obtained on an Agilent 1100 series LC/MSD spectrometer. Elemental analyses (C, H, N) were undertaken with Exeter Analytical Inc. Model CE-440 CHN analyzer.

### Synthesis

Chemical intermediates **6a-e** and **7a-e** and final compounds **8-22** (Scheme 1) were synthesized as per the literature procedure.[92,93]

**Synthesis of intermediates**

**General procedure for the preparation of 2-chloro-N-(4-aryl-substituted phenyl)acetamides 6a-e:**

To the stirring solution of 4-substituted anilines **5a-e** (0.039 mol) in anhydrous tetrahydrofuran (THF) maintained at 0-10°C, chloroacetyl chloride (0.05 mol) was added dropwise. This reaction mixture was then stirred at room temperature for about 7-8 h. After the completion of reaction, excess of THF was evaporated, and the resultant residue obtained was washed with water, filtered, and dried. Crude products **6a-e** thus obtained was then recrystallized using methanol.

*2-Chloro-N-(4-chlorophenyl)acetamide 6a:* IR (KBr, cm$^{-1}$): υ=737.34 (C-Cl str), 1247.85 (C-N str), 1670.49 (C=O str), 2952.71 (C-H aliphatic str), 3131.00 (C-H aromatic str), 3264.77 (N-H str); $^1$H NMR (CDCl$_3$, 400 MHz, ppm): δ=4.49 (s, 2H, CH$_2$), 7.36 (d, J = 7.2, 2H, Ar C-3, Ar C-5), 7.89 (d, J = 7.3, 2H, Ar C-2, Ar C-6), 8.25 (s, 1H, NH); $^{13}$C NMR (CDCl$_3$, 100 MHz, ppm): δ=44.39 (CH$_2$), 130.26 (Ar C-2, Ar C-6), 133.72 (Ar C-3, Ar C-5), 135.05 (Ar C-4), 139.18 (Ar C-1), 168.12 (C=O).

*2-Chloro-N-(4-fluorophenyl)acetamide 6b:* IR (KBr, cm$^{-1}$): υ=770.35 (C-Cl str), 1101.62 (C-F str), 1245.61 (C-N str), 1666.77 (C=O str), 2951.00 (C-H aliphatic str), 3129.43 (C-H aromatic str), 3274.96 (N-H str); $^1$H NMR (CDCl$_3$, 400 MHz, ppm): δ=4.52 (s, 2H, CH$_2$), 7.05 (d, J = 7.1, 2H, Ar C-3, Ar C-5), 7.91 (d, J = 7.4, 2H, Ar C-2, Ar C-6), 8.36 (s, 1H, NH); $^{13}$C NMR (CDCl$_3$, 100 MHz, ppm): δ=44.98 (CH$_2$), 120.18 (Ar C-3, Ar C-5), 129.46 (Ar C-2, Ar C-6), 138.40 (Ar C-1), 155.23 (Ar C-4), 166.54 (C=O).

*2-Chloro-N-(4-methoxyphenyl)acetamide 6c:* IR (KBr, cm$^{-1}$): υ=773.12 (C-Cl str), 1029.11 (C-N str), 1300.53 (C-O str), 1666.74 (C=O str), 2957.19 (C-H aliphatic str), 3136.10 (C-H aromatic str), 3295.74 (N-H str); $^1$H NMR (CDCl$_3$, 400 MHz, ppm): δ=3.93 (s, 3H, OCH$_3$), 4.48 (s, 2H, CH$_2$), 6.91 (d, J = 6.9, 2H, Ar C-3, Ar C-5), 7.85 (d, J = 7.2, 2H, Ar C-2, Ar C-6), 8.34 (s, 1H, NH); $^{13}$C NMR (CDCl$_3$, 100 MHz, ppm): δ=44.91 (CH$_2$), 56.71 (OCH$_3$), 117.54 (Ar C-3, Ar C-5), 126.12 (Ar C-2, Ar C-6), 133.80 (Ar C-1), 153.36 (Ar C-4), 168.37 (C=O).

*2-Chloro-N-p-tolylacetamide 6d:* IR (KBr, cm$^{-1}$): υ=765.84 (C-Cl str), 1027.16 (C-N str), 1667.75 (C=O str), 2956.00 (C-H aliphatic str), 3135.00 (C-H aromatic str), 3296.72 (N-H str); $^1$H NMR (CDCl$_3$, 400 MHz, ppm): δ=2.46 (s, 3H, CH$_3$), 4.43 (s, 2H, CH$_2$), 6.99 (d, J = 7.1, 2H, Ar C-3, Ar C-5), 7.68 (d, J = 7.3, 2H, Ar C-2, Ar C-6), 8.41 (s, 1H, NH); $^{13}$C NMR (CDCl$_3$, 100 MHz, ppm): δ=26.41 (CH$_3$), 46.30 (CH$_2$), 126.23 (Ar C-2, Ar C-6), 132.45 (Ar C-3, Ar C-5), 136.84 (Ar C-4), 139.48 (Ar C-1), 167.11 (C=O).

*2-Chloro-N-(4-nitrophenyl)acetamide 6e:* IR (KBr, cm$^{-1}$): υ=759.23 (C-Cl str), 1246.00 (C-N str), 1346.71, 1525.67 (NO$_2$ str), 1671.57 (C=O str), 2951.78 (C-H aliphatic str), 3129.45 (C-H aromatic str), 3265.98 (N-H str); $^1$H NMR (CDCl$_3$, 400 MHz, ppm): δ=4.53 (s, 2H, CH$_2$), 7.94 (d, J =

11

6.8, 2H, Ar C-2, Ar C-6), 8.36 (s, 1H, NH), 8.40 (d, $J$ = 7.1, 2H, Ar C-3, Ar C-5); $^{13}$C NMR (CDCl$_3$, 100 MHz, ppm): δ=45.62 (CH$_2$), 119.31 (Ar C-3, Ar C-5), 128.15 (Ar C-2, Ar C-6), 143.24 (Ar C-4), 146.32 (Ar C-1), 166.81 (C=O).

**General procedure for the preparation of 2-(4-aryl-substituted phenyl)iminothiazolidin-4-ones 7a-e:**

In the separate RB flasks containing respectively compounds **6a-e** (0.024 mol) dissolved in ethanol (30 mL), ammonium thiocyanate (0.098 mol) was added to each of them and the reaction mixtures were refluxed for about 4-5 h. After the completion of reaction, the reaction mixtures were left to stand overnight. The resultant precipitates **7a-e** so obtained was filtered, washed with water and recrystallized using methanol.

*2-(4-Chlorophenylimino)thiazolidin-4-one **7a**:* IR (KBr, cm$^{-1}$): υ=695.27 (C-S str), 737.79 (C-Cl str), 1241.61 (C-N str), 1567.23 (C=N str), 1674.11 (C=O str), 2925.72 (C-H aliphatic str), 3124.94 (C-H aromatic str), 3271.50 (N-H str); $^1$H NMR (CDCl$_3$, 400 MHz, ppm): δ=3.85 (s, 2H, thiazolidinone CH$_2$), 7.40 (d, $J$ = 7.2, 2H, Ar C-2, Ar C-4), 7.65 (d, $J$ = 7.3, 2H, Ar C-3, Ar C-5), 8.16 (s, 1H, thiazolidinone NH); $^{13}$C NMR (CDCl$_3$, 100 MHz, ppm): δ=34.37 (thiazolidinone CH$_2$), 125.32 (Ar C-2, Ar C-6), 133.14 (Ar C-3, Ar C-5), 136.23 (Ar C-4), 149.16 (Ar C-1), 165.74 (C=N), 176.91 (C=O).

*2-(4-Fluorophenylimino)thiazolidin-4-one **7b**:* IR (KBr, cm$^{-1}$): υ=701.95 (C-S str), 1143.69 (C-F str), 1262.90 (C-N str), 1565.36 (C=N str), 1687.58 (C=O str), 2931.20 (C-H aliphatic str), 3025.12 (C-H aromatic str), 3247.81 (N-H str); $^1$H NMR (CDCl$_3$, 400 MHz, ppm): δ=3.88 (s, 2H, thiazolidinone CH$_2$), 7.18 (d, $J$ = 7.2, 2H, Ar C-3, Ar C-5), 7.31 (d, $J$ = 7.3, 2H, Ar C-2, Ar C-4), 8.23 (s, 1H, thiazolidinone NH); $^{13}$C NMR (CDCl$_3$, 100 MHz, ppm): δ=35.19 (thiazolidinone CH$_2$), 119.93 (Ar C-3, Ar C-5), 126.81 (Ar C-2, Ar C-6), 147.53 (Ar C-1), 158.32 (Ar C-4), 165.11 (C=N), 175.80 (C=O).

*2-(4-Methoxyphenylimino)thiazolidin-4-one **7c**:* IR (KBr, cm$^{-1}$): υ=698.11 (CH$_3$ str), 703.85 (C-S str), 1246.21 (C-N str), 1281.30 (C-O str), 1572.38 (C=N str), 1670.15 (C=O str), 2952.06 (C-H aliphatic str), 3130.45 (C-H aromatic str), 3264.39 (N-H str); $^1$H NMR (CDCl$_3$, 400 MHz, ppm): δ=3.75 (s, 2H, thiazolidinone CH$_2$), 3.84 (s, 3H, OCH$_3$), 6.98 (d, $J$ = 6.9, 2H, Ar C-3, Ar C-5), 7.36 (d, $J$ = 7.1, 2H, Ar C-2, Ar C-4), 8.21 (s, 1H, thiazolidinone NH); $^{13}$C NMR (CDCl$_3$, 100 MHz, ppm): δ=35.72 (thiazolidinone CH$_2$), 56.95 (OCH$_3$), 117.24 (Ar C-3, Ar C-5), 128.46 (Ar C-2, Ar C-6), 144.32 (Ar C-1), 160.84 (Ar C-4), 165.21 (C=N), 175.29 (C=O).

*2-(p-Tolylimino)thiazolidin-4-one **7d**:* IR (KBr, cm$^{-1}$): υ=701.68 (C-S str), 1240.25 (C-N str), 1570.23 (C=N str), 1690.16 (C=O str), 2901.03 (C-H aliphatic str), 3097.12 (C-H aromatic str), 3399.00 (N-H str); $^1$H NMR (CDCl$_3$, 400 MHz, ppm): δ=2.41 (s, 3H, CH$_3$), 3.91 (s, 2H, thiazolidinone CH$_2$), 7.24 (d, $J$ = 7.0, 2H, Ar C-2, Ar C-4), 7.32 (d, $J$ = 7.1, 2H, Ar C-3, Ar C-5), 8.34 (s, 1H, thiazolidinone NH); $^{13}$C NMR (CDCl$_3$, 100 MHz, ppm): δ=25.19 (CH$_3$), 36.28 (thiazolidinone CH$_2$), 126.21 (Ar C-2, Ar C-6),

133.40 (Ar C-3, Ar C-5), 139.18 (Ar C-4), 148.36 (Ar C-1), 165.38 (C=N), 175.30 (C=O).

*2-(4-Nitrophenylimino)thiazolidin-4-one **7e**:* IR (KBr, cm$^{-1}$): υ=699.21 (C-S str), 1231.50 (C-N str), 1357.90, 1518.20 (NO$_2$ str), 1563.72 (C=N str), 1670.43 (C=O str), 2833.37 (C-H aliphatic str), 3006.76 (C-H aromatic str), 3204.78 (N-H str); $^1$H NMR (CDCl$_3$, 400 MHz, ppm): δ=3.84 (s, 2H, thiazolidinone CH$_2$), 7.69 (d, $J$ = 7.3, 2H, Ar C-2, Ar C-4), 8.20 (s, 1H, thiazolidinone NH), 8.46 (d, $J$ = 7.2, 2H, Ar C-3, Ar C-5); $^{13}$C NMR (CDCl$_3$, 100 MHz, ppm): δ=36.70 (thiazolidinone CH$_2$), 126.11 (Ar C-3, Ar C-5), 129.36 (Ar C-2, Ar C-6), 149.38 (Ar C-4), 156.25 (Ar C-1), 165.83 (C=N), 175.20 (C=O).

**Synthesis of final compounds 8-22**

The final compounds **8-22** were synthesized by the reaction of compounds **7a-e** (0.0022 mol) with appropriate heteroaryl-2-carbaldehydes *viz.* thiophene-2-carbaldehyde, furan-2-carbaldehyde and *1H*-imidazole-2-carbaldehyde (0.0049 mol) respectively in ethanol. The reaction mixture was heated until clear solution of reaction mixture was obtained, followed by addition of few drops of concentrated sulphuric acid and refluxed for 10-12 h. After the completion of reaction, the reaction mixtures were left to stand overnight. The resultant precipitates **8-22** so obtained were filtered, washed with water and recrystallized using methanol to produce final compounds **8-22**.

*2-(4-Chlorophenylimino)-5-(thiophen-2-ylmethylene)thiazolidin-4-one (**8**):* IR (KBr, cm$^{-1}$): υ=706.70 (C-S str), 756.24 (C-Cl str), 1232.21 (C-N str), 1539.93 (C=C aliphatic str), 1598.27 (C=C aromatic str), 1631.63 (C=N str), 1685.64 (C=O str), 2924.99 (C-H aliphatic str), 3053.02 (C-H aromatic str), 3244.96 (N-H str); $^1$H NMR (CDCl$_3$, 400 MHz, ppm): δ=7.21 (d, $J$ = 7.2, 2H, Ar C-2, Ar C-6), 7.31 (t, 1H, thiophene C-4), 7.35 (d, $J$ = 7.3, 2H, Ar C-3, Ar C-5), 7.42 (s, 1H, −C=CH), 7.62 (d, $J$ = 6.8, 1H, thiophene C-5), 7.66 (d, $J$ = 7.1, 1H, thiophene C-3), 8.02 (s, 1H, thiazolidinone NH); $^{13}$C NMR (CDCl$_3$, 100 MHz, ppm): δ=121.92, 142.21 (C=C), 123.75 (Ar C-2, Ar C-6), 127.13 (thiophene C-3), 128.21 (thiophene C-4), 130.21 (Ar C-3, Ar C-5), 131.52 (thiophene C-5), 132.80 (Ar C-4), 137.85 (thiophene C-2), 147.11 (Ar C-1), 163.32 (C=N), 168.58 (C=O); MS: *m/z*=319.18 [M]$^+$, 321.0 [M+2]; Anal. for C$_{14}$H$_9$ClN$_2$OS$_2$: calcd: C 52.41, H 2.83, N 8.73, found: C 52.49, H 2.80, N 8.77.

*2-(4-Fluorophenylimino)-5-(thiophen-2-ylmethylene)thiazolidin-4-one (**9**):* IR (KBr, cm$^{-1}$): υ=703.39 (C-S str), 1123.07 (C-F str), 1226.11 (C-N str), 1489.58 (C=C aliphatic str), 1551.32 (C=C aromatic str), 1613.59 (C=N str), 1669.54 (C=O str), 2954.24 (C-H aliphatic str), 3082.48 (C-H aromatic str), 3264.01 (N-H str); $^1$H NMR (CDCl$_3$, 400 MHz, ppm): δ=6.99 (d, $J$ = 7.0, 2H, Ar C-3, Ar C-5), 7.31 (d, $J$ = 7.2, 2H, Ar C-2, Ar C-6), 7.42 (t, 1H, thiophene C-4), 7.59 (s, 1H, −C=CH), 7.63 (d, $J$ = 6.7, 1H, thiophene C-5), 7.73 (d, $J$ = 7.1, 1H, thiophene C-3), 8.15 (s, 1H, thiazolidinone NH); $^{13}$C NMR (CDCl$_3$, 100 MHz, ppm): δ=121.85 (Ar C-3, Ar C-5), 121.99, 142.33 (C=C), 123.95 (Ar C-2, Ar C-6), 127.11 (thiophene C-3), 128.91 (thiophene C-4), 130.62 (thiophene C-5), 137.82 (thiophene C-2), 145.36 (Ar C-1), 159.13 (Ar C-4), 163.58 (C=N), 168.32

12

(C=O); MS: *m/z*=304.36 [M]$^+$, 306.0 [M+2]; Anal. for C$_{14}$H$_9$FN$_2$OS$_2$: calcd: C 55.25, H 2.98, N 9.20, found: C 55.20, H 3.02, N 9.18.

*2-(4-Methoxyphenylimino)-5-(thiophen-2-ylmethylene)thiazolidin-4-one (10):* IR (KBr, cm$^{-1}$): υ=701.28 (C-S str), 1228.19 (C-N str), 1310.27 (C-O str), 1490.59 (C=C aliphatic str), 1551.60 (C=C aromatic str), 1613.63 (C=N str), 1670.04 (C=O str), 2952.34 (C-H aliphatic str), 3082.5 (C-H aromatic str), 3284.78 (N-H str); $^1$H NMR (CDCl$_3$, 400 MHz, ppm): δ=3.68 (s, 3H, OCH$_3$), 6.89 (d, *J* = 6.7, 2H, Ar C-3, Ar C-5), 7.25 (d, *J* = 6.9, 2H, Ar C-2, Ar C-6), 7.29 (s, 1H, –C=CH), 7.39 (t, 1H, thiophene C-4), 7.57 (d, *J* = 6.8, 1H, thiophene C-5), 7.72 (d, *J* = 7.0, 1H, thiophene C-3), 8.17 (s, 1H, thiazolidinone NH); $^{13}$C NMR (CDCl$_3$, 100 MHz, ppm): δ=56.12 (OCH$_3$), 119.63 (Ar C-3, Ar C-5), 121.90, 144.13 (C=C), 123.93 (Ar C-2, Ar C-6), 128.10 (thiophene C-3), 132.41 (thiophene C-4), 135.18 (thiophene C-5), 136.28 (thiophene C-2), 145.02 (Ar C-1), 157.26 (Ar C-4), 163.45 (C=N), 168.27 (C=O); MS: *m/z*=316.0 [M]$^+$; Anal. for C$_{15}$H$_{12}$N$_2$O$_2$S$_2$: calcd: C 56.94, H 3.82, N 8.85, found: C 56.92, H 3.87, N 8.89.

*5-(Thiophen-2-ylmethylene)-2-(p-tolylimino)thiazolidin-4-one (11):* IR (KBr, cm$^{-1}$): υ=701.87 (C-S str), 1227.53 (C-N str), 1508.61 (C=C aliphatic str), 1593.53 (C=C aromatic str), 1623.54 (C=N str), 1687.53 (C=O str), 2934.54 (C-H aliphatic str), 3082.79 (C-H aromatic str), 3247.50 (N-H str); $^1$H NMR (CDCl$_3$, 400 MHz, ppm): δ=2.43 (s, 3H, CH$_3$), 6.99 (d, *J* = 6.9, 2H, Ar C-3, Ar C-5), 7.18 (d, *J* = 7.1, 2H, Ar C-2, Ar C-6), 7.37 (t, 1H, thiophene C-4), 7.46 (s, 1H, –C=CH), 7.63 (d, *J* = 6.6, 1H, thiophene C-3), 7.69 (d, *J* = 6.7, 1H, thiophene C-5), 8.19 (s, 1H, thiazolidinone NH); $^{13}$C NMR (CDCl$_3$, 100 MHz, ppm): δ=25.73 (CH$_3$), 120.87, 126.38 (thiophene C-3), 124.52 (Ar C-2, Ar C-6), 130.12 (thiophene C-4), 131.65 (Ar C-3, Ar C-5), 133.25 (thiophene C-5), 137.91 (thiophene C-2), 138.08 (Ar C-4), 143.52 (C=C), 147.03 (Ar C-1), 167.24 (C=O), 162.95 (C=N); MS: *m/z*=300.1 [M]$^+$; Anal. for C$_{15}$H$_{12}$N$_2$OS$_2$: calcd: C 59.97, H 4.03, N 9.33, found: C 60.02, H 4.08, N 9.30.

*2-(4-Nitrophenylimino)-5-(thiophen-2-ylmethylene)thiazolidin-4-one (12):* IR (KBr, cm$^{-1}$): υ=702.45 (C-S str), 1216.59 (C-N str), 1325.81, 1527.34 (NO$_2$ str), 1549.49 (C=C aromatic str), 1589.00 (C=C aliphatic str), 1606.02 (C=N str), 1660.94 (C=O str), 2954.53 (C-H aliphatic str), 3061.84 (C-H aromatic str), 3293.60 (N-H str); $^1$H NMR (CDCl$_3$, 400 MHz, ppm): δ=7.33 (t, 1H, thiophene C-4), 7.50 (s, 1H, –C=CH), 7.66 (d, *J* = 7.3, 1H, thiophene C-5), 7.78 (d, *J* = 7.0, 1H, thiophene C-3), 7.85 (d, *J* = 7.4, 2H, Ar C-2, Ar C-6), 8.23 (s, 1H, thiazolidinone NH), 8.37 (d, *J* = 7.2, 2H, Ar C-3, Ar C-5); $^{13}$C NMR (CDCl$_3$, 100 MHz, ppm): δ=120.89, 143.23 (C=C), 124.19 (Ar C-3, Ar C-5), 127.35 (Ar C-2, Ar C-6), 129.10 (thiophene C-3), 132.23 (thiophene C-4), 136.53 (thiophene C-5), 136.89 (thiophene C-2), 148.24 (Ar C-4), 149.92 (Ar C-1), 162.16 (C=N), 166.99 (C=O); MS: *m/z*=332.0 [M]$^+$; Anal. for C$_{14}$H$_9$N$_3$O$_3$S$_2$: calcd: C 50.74, H 2.74, N 12.68, found: C 50.70, H 2.73, N 12.60.

*2-(4-Chlorophenylimino)-5-(furan-2-ylmethylene)thiazolidin-4-one (13):* IR (KBr, cm$^{-1}$): υ=704.32 (C-S str), 756.72 (C-Cl str), 1223.37 (C-N str), 1310.03 (C-O str), 1508.77 (C=C aliphatic str), 1566.68 (C=C aromatic str), 1626.31 (C=N str),1669.62 (C=O str), 2950.01 (C-H aliphatic str), 3123.12 (C-H aromatic str), 3274.04 (N-H str); $^1$H NMR (CDCl$_3$, 400 MHz,

ppm): δ=6.40 (t, 1H, thiophene C-4), 7.01 (d, *J* = 7.4, 1H, thiophene C-3), 7.18 (d, *J* = 7.3, 2H, Ar C-3, Ar C-5), 7.20 (d, *J* = 7.1, 2H, Ar C-2, Ar C-6), 7.38 (s, 1H, –C=CH), 7.43 (d, *J* = 7.2, 1H, thiophene C-5), 8.21 (s, 1H, thiazolidinone NH); $^{13}$C NMR (CDCl$_3$, 100 MHz, ppm): δ=115.34 (furan C-3), 118.56 (furan C-4), 121.89, 144.93 (C=C), 123.74 (Ar C-2, Ar C-6), 132.01 (Ar C-3, Ar C-5), 134.23 (Ar C-4), 140.87 (furan C-5), 147.38 (Ar C-1), 154.08 (furan C-2), 163.22 (C=N), 168.35 (C=O); MS: *m/z*=304.0 [M]$^+$, 306.3 [M+2]; Anal. for C$_{14}$H$_9$ClN$_2$O$_2$S: calcd: C 56.94, H 3.82, N 8.85, found: C 56.92, H 3.87, N 8.89.

*2-(4-Fluorophenylimino)-5-(furan-2-ylmethylene)thiazolidin-4-one (14):* IR (KBr, cm$^{-1}$): υ=702.16 (C-S str), 1124.36 (C-F str), 1225.32 (C-N str), 1313.54 (C-O str), 1487.26 (C=C aliphatic str), 1545.60 (C=C aromatic str), 1625.15 (C=N str),1662.35 (C=O str), 2923.25 (C-H aliphatic str), 3119.09 (C-H aromatic str), 3292.71 (N-H str); $^1$H NMR (CDCl$_3$, 400 MHz, ppm): δ=6.58 (t, 1H, furan C-4), 6.99 (d, *J* = 7.0, 1H, furan C-3), 7.19 (d, *J* = 7.2, 2H, Ar C-2, Ar C-6), 7.28 (d, *J* = 7.2, 2H, Ar C-3, Ar C-5), 7.42 (s, 1H, –C=CH), 7.92 (d, *J* = 7.4, 1H, furan C-5), 8.07 (s, 1H, thiazolidinone NH); $^{13}$C NMR (CDCl$_3$, 100 MHz, ppm): δ=110.68 (furan C-4), 113.25 (furan C-3), 119.45 (Ar C-3, Ar C-5), 121.90, 143.71 (C=C), 124.56 (Ar C-2, Ar C-6), 144.04 (furan C-5), 146.37 (Ar C-1), 152.61 (furan C-2), 159.95 (Ar C-4), 163.17 (C=N), 168.12 (C=O); MS: *m/z*=288.6 [M]$^+$, 290.3 [M+2]; Anal. for C$_{14}$H$_9$FN$_2$O$_2$S: calcd: C 58.33, H 3.15, N 9.72, found: C 58.32, H 3.19, N 9.69.

*5-(Furan-2-ylmethylene)-2-(4-methoxyphenylimino)thiazolidin-4-one (15):* IR (KBr, cm$^{-1}$): υ=701.25 (C-S str), 1223.12 (C-N str), 1311.64 (C-O str), 1627.14 (C=N str), 1514.90 (C=C aliphatic str), 1548.13 (C=C aromatic str), 1675.19 (C=O str), 2979.25 (C-H aliphatic str), 3083.28 (C-H aromatic str), 3372.96 (N-H str); $^1$H NMR (CDCl$_3$, 400 MHz, ppm): δ=3.68 (s, 3H, OCH$_3$), 6.57 (d, *J* = 6.9, 2H, Ar C-3, Ar C-5), 6.71 (t, 1H, furan C-4), 7.03 (d, *J* = 6.8, 1H, furan C-3), 7.23 (d, *J* = 7.0, 2H, Ar C-2, Ar C-6), 7.37 (s, 1H, –C=CH), 7.95 (d, *J* = 7.3, 1H, furan C-5), 8.31 (s, 1H, thiazolidinone NH); $^{13}$C NMR (CDCl$_3$, 100 MHz, ppm): δ=54.37 (OCH$_3$), 110.77 (Ar C-3, Ar C-5), 114.21 (furan C-3), 115.43 (furan C-4), 122.95, 143.09 (C=C), 124.26 (Ar C-2, Ar C-6), 142.15 (Ar C-1), 146.03 (furan C-5), 152.99 (furan C-2), 158.63 (Ar C-4), 163.34 (C=N), 168.15 (C=O); MS: *m/z*=300.7 [M]$^+$; Anal. for C$_{15}$H$_{12}$N$_2$O$_3$S: calcd: C 59.99, H 4.03, N 9.33, found: C 60.03, H 4.08, N 9.30.

*5-(Furan-2-ylmethylene)-2-(p-tolylimino)thiazolidin-4-one (16):* IR (KBr, cm$^{-1}$): υ=703.58 (C-S str), 1265.02 (C-N str), 1315.22 (C-O str), 1537.87 (C=C aliphatic str), 1594.34 (C=C aromatic str), 1607.80 (C=N str), 1665.69 (C=O str), 2995.54 (C-H aliphatic str), 3073.68 (C-H aromatic str), 3303.92 (N-H str); $^1$H NMR (CDCl$_3$, 400 MHz, ppm): δ=2.46 (s, 3H, CH$_3$), 6.75 (t, 1H, furan C-4), 7.05 (d, *J* = 6.8, 1H, furan C-3), 7.14 (d, *J* = 7.3, 2H, Ar C-2, Ar C-6), 7.22 (d, *J* = 7.2, 2H, Ar C-3, Ar C-5), 7.39 (s, 1H, –C=CH), 7.86 (d, *J* = 7.3, 1H, furan C-5), 8.11 (s, 1H, thiazolidinone NH); $^{13}$C NMR (CDCl$_3$, 100 MHz, ppm): δ=26.31 (CH$_3$), 113.33 (furan C-3), 116.41 (furan C-4), 121.38, 143.30 (C=C), 123.68 (Ar C-2, Ar C-6), 132.82 (Ar C-3, Ar C-5), 138.71 (Ar C-4), 145.94 (furan C-5), 148.15 (Ar C-1), 151.92 (furan C-2), 164.32 (C=N), 167.97 (C=O); MS: *m/z*=285.0 [M]$^+$; Anal. for C$_{15}$H$_{12}$N$_2$O$_2$S: calcd: C 63.36, H 4.25, N 9.85, found: C 63.39, H 4.27, N 9.80.

13

*5-(Furan-2-ylmethylene)-2-(4-nitrophenylimino)thiazolidin-4-one* **(17)**: IR (KBr, cm$^{-1}$): υ=704.39 (C-S str), 1223.16 (C-N str), 1310.08 (C-O str), 1328.45, 1526.74 (NO$_2$ str), 1545.63 (C=C aliphatic str), 1595.20 (C=C aromatic str), 1632.21 (C=N str),1664.63 (C=O str), 2929.19 (C-H aliphatic str), 3126.78 (C-H aromatic str), 3304.41 (N-H str); $^1$H NMR (CDCl$_3$, 400 MHz, ppm): δ=6.83 (t, 1H, furan C-4), 7.13 (d, *J* = 7.5, 1H, furan C-3), 7.42 (s, 1H, −C=CH), 7.55 (d, *J* = 7.1, 2H, Ar C-2, Ar C-6), 7.87 (d, *J* = 7.2, 2H, Ar C-3, Ar C-5), 7.92 (d, *J* = 7.3, 1H, furan C-5), 8.23 (s, 1H, thiazolidinone NH); $^{13}$C NMR (CDCl$_3$, 100 MHz, ppm): δ=111.65 (furan C-3), 114.17 (furan C-4), 120.02 (Ar C-3, Ar C-5), 121.65, 143.43 (C=C), 122.57 (Ar C-2, Ar C-6), 137.35 (Ar C-4), 144.57 (furan C-5), 151.26 (Ar C-1), 152.05 (furan C-2), 163.47 (C=N), 168.28 (C=O); MS: *m/z*=315.0 [M]$^+$; Anal. for C$_{14}$H$_9$N$_3$O$_4$S: calcd: C 53.33, H 2.88, N 13.33, found: C 53.29, H 2.93, N 13.31.

*((1H-imidazol-2-yl)methylene)-2-(4-chlorophenylimino)thiazolidin-4-one* **(18)**: IR (KBr, cm$^{-1}$): υ=702.16 (C-S str), 763.18 (C-Cl str), 1227.01 (C-N str), 1539.04 (C=C aromatic str), 1603.66 (C=C aliphatic str), 1627.12 (C=N str), 1669.63 (C=O str), 2924.85 (C-H aliphatic str), 3192.85 (C-H aromatic str), 3303.93 (N-H str); $^1$H NMR (CDCl$_3$, 400 MHz, ppm): δ=7.15 (t, 1H, imidazole C-4), 7.24 (d, *J* = 7.4, 1H, imidazole C-5), 7.35 (s, 1H, −C=CH), 7.53 (d, *J* = 7.2, 2H, Ar C-2, Ar C-6), 7.64 (d, *J* = 7.3, 2H, Ar C-3, Ar C-5), 8.17 (s, 1H, thiazolidinone NH), 9.45 (s, 1H, imidazole NH); $^{13}$C NMR (CDCl$_3$, 100 MHz, ppm): δ=110.97 (Ar C-3, Ar C-5), 121.59, 143.85 (C=C), 124.15 (Ar C-2, Ar C-6), 129.37 (imidazole C-4), 131.28 (imidazole C-5), 135.08 (Ar C-4), 136.63 (imidazole C-2), 145.31 (Ar C-1), 163.39 (C=N), 168.74 (C=O); MS: *m/z*=304.0 [M]$^+$, 306.5 [M+2]; Anal. for C$_{13}$H$_9$ClN$_4$OS: calcd: C 51.23, H 2.98, N 18.38, found: C 51.26, H 2.99, N 18.30.

*5-((1H-imidazol-2-yl)methylene)-2-(4-fluorophenylimino)thiazolidin-4-one* **(19)**: IR (KBr, cm$^{-1}$): υ=701.42 (C-S str), 1120.13 (C-F str), 1222.98 (C-N str), 1559.40 (C=C aromatic str), 1581.63 (C=C aliphatic str), 1623.31 (C=N str), 1669.54 (C=O str), 2925.60 (C-H aliphatic str), 3137.30 (C-H aromatic str), 3305.23 (N-H str); $^1$H NMR (CDCl$_3$, 400 MHz, ppm): δ=6.98 (d, *J* = 7.2, 2H, Ar C-3, Ar C-5), 7.18 (d, *J* = 7.0, 2H, Ar C-2, Ar C-6), 7.23 (t, 1H, imidazole C-4), 7.31 (d, *J* = 7.3, 1H, imidazole C-5), 7.45 (s, 1H, −C=CH), 8.26 (s, 1H, thiazolidinone NH), 9.42 (s, 1H, imidazole NH); $^{13}$C NMR (CDCl$_3$, 100 MHz, ppm): δ=115.25 (Ar C-3, Ar C-5), 122.91, 141.87 (C=C), 124.03 (Ar C-2, Ar C-6), 126.86 (imidazole C-4), 130.19 (imidazole C-5), 136.52 (imidazole C-2), 145.16 (Ar C-1), 158.01 (Ar C-4), 163.24 (C=N), 168.43 (C=O); MS: *m/z*=304.4 [M]$^+$, 306.7 [M+2]; Anal. for C$_{13}$H$_9$FN$_4$OS: calcd: C 54.16, H 3.15, N 19.43, found: C 54.20, H 3.11, N 19.41.

*5-((1H-imidazol-2-yl)methylene)-2-(4-methoxyphenylimino)thiazolidin-4-one (20)*: IR (KBr, cm$^{-1}$): υ=700.99 (C-S str), 1225.36 (C-N str), 1538.43 (C=C aromatic str), 1595.96 (C=C aliphatic str), 1621.42 (C=N str), 1684.94 (C=O str), 2924.86 (C-H aliphatic str), 3053.70 (C-H aromatic str), 3248.56 (N-H str); $^1$H NMR (CDCl$_3$, 400 MHz, ppm): δ=3.42 (s, 3H, OCH$_3$), 6.78 (d, *J* = 7.1, 2H, Ar C-3, Ar C-5), 7.11 (d, *J* = 6.9, 1H, imidazole C-5), 7.23 (t, 1H, imidazole C-4), 7.38 (s, 1H, −C=CH), 7.50 (d, *J* = 7.2, 2H, Ar C-2, Ar C-6), 8.22 (s, 1H, thiazolidinone NH), 9.76 (s, 1H, imidazole NH); $^{13}$C NMR (CDCl$_3$, 100 MHz, ppm): δ=54.84 (OCH$_3$), 112.54 (Ar C-3, Ar C-5), 121.93, 142.98 (C=C), 124.32 (Ar C-2, Ar C-6), 129.21 (imidazole C-4), 131.40 (imidazole C-5), 136.14 (imidazole C-2), 143.08 (Ar C-1), 150.24 (Ar C-4), 163.48 (C=N), 168.62 (C=O); MS: *m/z*=300.8 [M]$^+$; Anal. for C$_{14}$H$_{12}$N$_4$O$_2$S: calcd: C 55.99, H 4.03, N 18.65, found: C 56.04, H 4.01, N 18.62.

*5-((1H-imidazol-2-yl)methylene)-2-(p-tolylimino)thiazolidin-4-one* **(21)**: IR (KBr, cm$^{-1}$): υ=701.39 (C-S str), 1224.17 (C-N str), 1544.05 (C=C aliphatic str), 1596.12 (C=C aromatic str), 1641.79 (C=N str), 1665.23 (C=O str), 2924.86 (C-H aliphatic str), 3058.17 (C-H aromatic str), 3303.51 (N-H str); $^1$H NMR (CDCl$_3$, 400 MHz, ppm): δ=2.43 (s, 3H, CH$_3$), 7.25 (t, 1H, imidazole C-4), 7.32 (d, *J* = 6.9, 1H, imidazole C-5), 7.40 (d, *J* = 7.2, 2H, Ar C-3, Ar C-5), 7.43 (s, 1H, −C=CH), 7.56 (d, *J* = 7.3, 2H, Ar C-2, Ar C-6), 8.29 (s, 1H, thiazolidinone NH), 9.38 (s, 1H, imidazole NH); $^{13}$C NMR (CDCl$_3$, 100 MHz, ppm): δ=25.82 (CH$_3$), 121.45, 142.63 (C=C), 127.43 (Ar C-2, Ar C-6), 129.48 (imidazole C-4), 131.23 (Ar C-3, Ar C-5), 131.37 (imidazole C-5), 135.61 (Ar C-4), 136.75 (imidazole C-2), 145.90 (Ar C-1), 163.21 (C=N), 168.53 (C=O); MS: *m/z*=283.3 [M]$^+$; Anal. for C$_{14}$H$_{12}$N$_4$OS: calcd: C 59.14, H 4.25, N 19.70, found: C 59.13, H 4.29, N 19.77.

*5-((1H-imidazol-2-yl)methylene)-2-(4-nitrophenylimino)thiazolidin-4-one* **(22)**: IR (KBr, cm$^{-1}$): υ=701.45 (C-S str), 1226.17 (C-N str), 1331.83, 1556.56 (NO$_2$ str), 1489.00 (C=C aliphatic str), 1549.50 (C=C aromatic str), 1606.02 (C=N str), 1660.94 (C=O str), 2924.03 (C-H aliphatic str), 3059.14 (C-H aromatic str), 3293.60 (N-H str); $^1$H NMR (CDCl$_3$, 400 MHz, ppm): δ=7.18 (t, 1H, imidazole C-4), 7.25 (d, *J* = 7.3, 1H, imidazole C-5), 7.41 (s, 1H, −C=CH), 7.61 (d, *J* = 6.8, 2H, Ar C-2, Ar C-6), 7.92 (d, *J* = 7.2, 2H, Ar C-3, Ar C-5), 8.21 (s, 1H, thiazolidinone NH), 9.67 (s, 1H, imidazole NH); $^{13}$C NMR (CDCl$_3$, 100 MHz, ppm): δ=119.58 (Ar C-3, Ar C-5), 121.43, 143.57 (C=C), 123.48 (Ar C-2, Ar C-6), 128.35 (imidazole C-4), 130.81 (imidazole C-5), 135.64 (imidazole C-2), 139.52 (Ar C-4), 145.54 (Ar C-1), 163.74 (C=N), 168.32 (C=O); MS: *m/z*=314.0 [M]$^+$; Anal. for C$_{13}$H$_9$N$_5$O$_3$S: calcd: C 49.52, H 2.88, N 22.21, found: C 49.46, H 2.92, N 22.20.

**PTP1B inhibition assay**

The final compounds **8-22** were evaluated for *in-vitro* PTP1B inhibitory activity using *Calbiochem PTP1B Colorimetic Assay Kit* (Calbiochem PTP1B Assay Kit, Colorimetric, User Protocol. 2008, Catalogue No: 539736).[94] The kit consisted of human recombinant PTP1B (residues 1-322; MW 37,400), expressed in *E.coli*.

The test is based on the principle that PTP1B hydrolyzes the IR5 phosphopeptide substrate (IR5 phosphopeptide substrate contains sequence from the insulin receptor β subunit domain that must be autophosphorylated to achieve full receptor kinase activation. This "activation loop" is the target of protein phosphatase regulators of insulin signalling, notably PTP1B) resulting in the release of the free phosphate which is detected in terms of absorbance values at wavelength of 620 nm.

The experiments were carried out under all suitable laboratory conditions according to the manufacturer's protocol. The test compounds **8-22** were

14

dissolved in DMSO to prepare the test solutions and suramin was taken as a reference. To test PTP1B inhibition activity of test compounds, an aliquot was made to contain mixture of 35 µl assay buffer (300 mM NaCl, 100 mM MES, 2 mM DTT, 2 mM EDTA, 0.1% NP-40, pH 7.2) warmed to assay temperature i.e. 30°C, 10 µl solubilizing solution (control or inhibitor solution at five different concentrations) and 5 µl diluted PTP1B enzyme (human recombinant PTP1B consisting of residues 1-322; MW 37400), expressed in *E.coli* 100 ng/ µl in 50 mM HEPES, 1 mM EDTA, 1 MM DTT, 10% v/v glycerol, 0.05% NP-40, pH 7.2). The reaction was then initiated by adding 50 µl of the warmed PTP1B substrate (IR5, composed of amino acids 1142-1153, pY1146, MW 1703 kDa). The mixture was incubated for 30 minutes at 30°C. The reaction was terminated by the addition of 25 µl of Red Reagent (phosphate detection reagent). The mixture was then agitated and allowed to stand for about 30 minutes to develop color. The absorbance was measured at 620 nm using Bio-Rad 680XR microplate reader. Control experiments were carried out without inhibitor and blanks were run without PTP1B enzyme. All the assays were performed in duplicate. $IC_{50}$ values were calculated, along with the 95% confidence limits, with GraphPad Prism Software (version 5.0), using plots of inhibition percentages (calculated in relation to a sample of the enzyme treated under the same conditions without inhibitors) versus the logarithm of the inhibitor concentration. Additionally, it is important to state here that all the synthesized compounds were subjected to UV-visible spectral analysis and none of the compounds absorbed in the wavelength of 620 nm used in the PTP1B inhibition assay.

### Kinetic measurements of lead PTP1B inhibitor 17

In order to perform the kinetic characterization of PTP1B, the most promising inhibitor, compound **17** in different concentrations (5 µM, 10 µM, 20 µM) was preincubated with the enzyme, assay buffer, and PTP1B substrate at 30°C. Kinetic characterization of the hydrolysis of the IR5 phosphopeptide substrate catalyzed by PTP1B was recorded at 620 nm. A parallel control was made for an assay solution with no inhibitor. The plots were assessed by a weighed least square analysis that assumed the variance of V to be a constant percentage of V for the entire data set. The Lineweaver-Burk plots (reciprocal plot slopes) were plotted as a function of the concentrations of the inhibitors in a weighted analysis.

### Molecular modeling simulations

Molecular docking simulations were conducted on the synthesized compounds **8-22** using the AutoDock 4.2 to get insight about their binding preferences within the active site of the receptor. The molecular docking simulations were performed on the PC based machines running on Windows 7 (x86) as operating system. The software included MGL tools 1.5.4 based AutoDock 4.2 (www.scripps.edu) which uses Python 2.7 language - Cygwin C:\ program (www.cygwin.com) and Python 2.5 (www.python.com). The docked molecules within the PTP1B active site were visualized using Discovery Studio Visualizer 3.1 (www.accelrys.com).

### Preparation of coordinate file

The X-ray crystal structure of human PTP1B complexed with an inhibitor, 4-bromo-3-(carboxymethoxy)-5-[3-(cyclohexylamino)phenyl]thiophene-2-carboxylic acid (PDB entry: 2QBS, resolution = 2.1 Å) was retrieved from Protein Data Bank (https:/www.rscb.org/pdb) (Douglas et al., 2007). The protein structure was prepared using the Discovery Studio Visualizer (version 3.1) and AutoDock Tools (ADT; version 1.5.4) through different steps *viz.* removal of water molecules and co-crystallized ligand, addition of missing hydrogen atoms, addition of Gasteiger-Marsili and Kollman charges, merging of non-polar hydrogens, and assignment of rotatable bonds. The file was then saved to pdbqt file format for further analysis.

### Preparation of ligands

The chemical structures of compounds **8-22** and reference inhibitor (BTC, 4-Bromo-3-(carboxymethoxy)-5-[3-(cyclohexylamino)phenyl]thiophene-2-carboxylic acid) were constructed using Chem3D 15.0 module of ChemOffice 15.0 and saved in PDB format. The structures were optimized using "Prepare Ligands" in the AutoDock 4.2, flexible torsions were assigned, the acyclic dihedral angles were allowed to rotate freely and the file was then saved as pdbqt file format for further analysis.

### Docking Methodology

The flexible docking was performed using the refined protein molecule, 2QBS, for PTP1B according to the previously reported protocol.[95] The grid maps of the interaction energies of various atom types were pre-calculated using AutoGrid 4.2. In each docking, a grid box was created using a grid map of 45×45×45 points and a grid spacing of 0.375 Å. The grid maps were centered on the corresponding ligand binding site within the protein structure. Lamarckian Genetic Algorithm (LGA) was adopted to perform docking simulations using the following default parameters, *viz.* 100 independent runs with step sizes of 0.2 Å for translations and 5 Å for orientations and torsions, an initial population of random individuals with a population size of 150 individuals, a maximum of 2.5 x $10^6$ energy evaluations, maximum number of generations of 27,000; mutation and crossover rates of 0.02 and 0.8 respectively; and an elitism value of 1. All the computations were carried out on Cygwin and was used to generate both grid parameter file (.gpf file) and docking parameter file (.dpf file) for each ligand. The docked conformations of each ligand were ranked into clusters based on the binding energy and the top ranked conformations were used for further study. The pose with lowest ΔG-score was considered the best fitted one and was further analyzed for ligand-receptor interactions.

### *In-silico* drug-likeness and pharmacokinetic property prediction

The *in-silico* prediction studies were performed using pkCSM and and ProTox online prediction platforms which helps to assess the theoretical pharmacokinetic parameters of the ligands to predict the drug-likeness of ligands. The software calculated pharmaceutically relevant properties such as H-bond donor, H-bond acceptor, octanol-water partition coefficient (LogP), surface area, number of rotatable bonds, in addition to the effect of ligands on ADME parameters like water solubility, Caco2 permeability, human intestinal absorption, skin permeability, P-

15

**FULL PAPER**

glycoprotein I and II inhibition, volume of distribution, fraction of unbound drug, BBB and CNS permeability, cytochrome P450 (CYP3A4 and CYP2C9 inhibition) inhibition, total clearance, action as renal OCT2 (organic cation transporter 2) substrate; and on toxicity parameters like AMES toxicity, hERG I and II inhibition, oral rat acute toxicity, oral rat chronic toxicity, hepatotoxicity, skin sensitization, *T.pyriformis* and minnow toxicity, cytotoxicity, and assessment of maximum recommended tolerated dose.

## Acknowledgements

## Disclosure statement

No potential conflict of interest has been reported by the authors.

**Keywords:** Diabetes • protein tyrosine phosphatase 1B (PTP1B) inhibitors • thiazolidin-4-ones • molecular docking • pharmacokinetic studies

## References

[1]     J. S. Skyler, *J. Med. Chem.* **2004**, 47, 4113-4117.

[2]     A. T. Kharroubi, H. M. Darwish, *World J. Diabetes.* **2015**, 6, 850-867.

[3]     (a) International Diabetes Federation. IDF Diabetes Atlas – 9th Edition 2019. [Available from www.diabetesatlas.org.] (b) P. Saeedi, I. Petersohn, P. Salpea, B. Malanda, S. Karuranga, N. Unwin, S. Colagiuri, L. Guariguata, A. A. Motala, K. Ogurtsova, J. E. Shaw, D. Bright, R. Williams, On behalf of the IDF Diabetes Atlas Committee, *Diabetes Res. Clin. Pract.* **2019**, 157, 107843-107852.

[4]     C. D. Mathers, D. Loncar, *PLoS Med.* **2006**, 3, e442.

[5]     S. A. Ross, E. A. Gulve, M. Wang, *Chem. Rev.* **2004**, 104, 1255-1282.

[6]     American Diabetes Association. *Diabetes Care.* **2009**, 32(Suppl 1), S62-S67.

[7]     A. R. Saltiel, J. E. Pessin, *Trends Cell Biol.* **2002**, 12, 65-71.

[8]     S. Del Prato, N. Pulizzi, *Metabolism* **2006**, 55, S20-S27.

[9]     G. Shammi, K. R. Jitendra, R. K. Narang, K. S. Rajesh, *Int. J. Pharm. Pharm. Sci.* **2010**, 2, 1-6.

[10]    G. A. R. Y. Suaifan, M. B. Shehadeh, R. M. Darwish, H. Al-Ijel, V. Abbate, *Molecules* **2015**, 20, 20063-20078.

[11]    T. O. Johnson, J. Ermolieff, M. R. Jirousek, *Nat. Rev. Drug Discov.* 2001, 1, 696-709.

[12]    T. Hunter, *Cell* **2000**, 100, 113-127.

[13]    A. Bononi, C. Agnoletto, E. D. Marchi, S. Marchi, S. Patergnani, M. Bonora, C. Giorgi, F. Poletti, A. Rimessi, P. Pinton, *Enzyme Res.* **2011**, 2011, 329098.

[14]    M. J. Lee, M. B. Yaffe. *Cold Spring Harb. Perspect. Biol.* **2016**, 8, a005918.

[15]    S. M. Stanford, N. Rapini, N. Bottini, *Immunology* **2012**, 137, 1-19.

[16]    T. E. Taher, J. Bystrom, V. H. Ong, D. A. Isenberg, Y. Renaudineau, D. J. Abraham, R. A. Mageed, *Clin Rev. Allergy Immunol.* **2017**, 5, 237-264.

[17]    R. Majeti, A. Weiss, *Chem. Rev.* **2001**, 101, 2441-2448.

[18]    J. K. Lassila, J. G. Zalatan, D. Herschlag, *Annu Rev Biochem.* **2011**, 80, 669-702.

[19]    A. Pabis, D. Duarte, S. C. L. Kamerlin, *Biochemistry* **2016**, 55, 3061-3081.

[20]    Z. Y. Zhang, *Annu. Rev. Pharmacol. Toxicol.* **2002**, 42, 209-234.

[21]    H. Nishi, K. Hashimoto, A. R. Panchenko, *Structure.* **2011**, 19, 1807-1815.

[22]    D. Van Vactor, A. M. O'Reilly, B. G. Neel, *Curr. Opin. Genet. Dev.* **1998**, 8, 112-126.

[23]    N. K. Tonks, *FEBS J.* **2013**, 280, 346-378.

[24]    F. Ardito, M. Giuliani, D. Perrone, G. Troiano, L. L. Muzio, *Int. J. Mol. Med.* **2017**, 40, 271-280.

[25]    Z.-H. Yu, Z.-Y. Zhang, *Chem. Rev.* **2018**, 118, 1069-1091.

[26]    Z. Y. Zhang, *Crit. Rev. Biochem. Mol. Biol.* **1998**, 33(1), 1-52.

[27]    T. K. B. Gandhi, S. Chandran, S. Peri, R. Saravana, R. Amanchy, T. S. K. Prasad, A. Pandey, *DNA Res.* **2005**, 12, 79-89.

[28]    R. J. He, Z. H. Yu, R. Y. Zhang, Z. Y. Zhang, *Acta Pharmacol. Sin.* **2014**, 35, 1227-1246.

[29]    R. H. Reddy, H. Kim, S. Cha, B. Lee, Y. J. Kim, *J. Microbiol. Biotechnol.* **2017**, 27, 878-895.

[30]    L. Li, J. E. Dixon, *Semin. Immunol.* **2000**, 12, 75-84.

[31]    T. Kaneko, R. Joshi, S. M. Feller, S. S. C. Li, *Cell Commun. Signal.* **2012**, 10, 32-51.

[32]    M. J. Wagner, M. M. Stacey, B. A. Liu, T. Pawson, *Cold Spring Harb. Perspect. Biol.* **2013**, 5, a008987.

[33]    Z. Y. Zhang, *Curr. Opin. Chem. Biol.* **2001**, 5, 416-423.

[34]    J. Ma, Z. Li, S. Xing, W. T. Ho, X. Fu, Z. J. Zhao, *Biochem. Biophys. Res. Commun.* **2011**, 407, 98–102.

[35]    R. C. Sharp, M. Abdulrahim, E. S. Naser, S. A. Naser, *Front. Cell Infect. Microbiol.* **2015**, 5, 95.

[36]    U. Lorenz, *Immunol. Rev.* **2009**, 228, 342-359.

[37]    D. Barford, A. K. Das, M. P. Egloff, *Annu. Rev. Biophys. Biomol. Struct.* **1998**, 27, 133-164.

[38]    E. S. Lander, L. M. Linton, B. Birren, C. Nusbaum, M. C. Zody, J. Baldwin, K. Devon, K. Dewar, M. Doyle, W. FitzHugh, R. Funke, D. Gage, K. Harris, A. Heaford, J. Howland, L. Kann, J. Lehoczky, R. LeVine, P. McEwan, K. McKernan, J. Meldrim, J.P. Mesirov, C. Miranda, W. Morris, J. Naylor, C. Raymond, M. Rosetti, R. Santos, A. Sheridan, C. Sougnez, N. Stange-Thomann, N. Stojanovic, A. Subramanian, D. Wyman, J. Rogers, J. Sulston, R. Ainscough, S. Beck, D. Bentley, J. Burton, C. Clee, N. Carter, A. Coulson, R. Deadman, P. Deloukas, A. Dunham, I. Dunham, R. Durbin, L. French, D. Grafham, S. Gregory, T. Hubbard, S. Humphray, A. Hunt, M. Jones, C. Lloyd, A. McMurray, L. Matthews, S. Mercer, S. Milne, J. C. Mullikin, A. Mungall, R. Plumb, M. Ross, R. Shownkeen, S. Sims, R. H. Waterston, R. K. Wilson, L. W. Hillier, J. D. McPherson, M. A. Marra, E. R. Mardis, L. A. Fulton, A. T. Chinwalla, K. H. Pepin, W. R. Gish, S. L. Chissoe, M. C. Wendl, K. D. Delehaunty, T. L. Miner, A. Delehaunty, J. B. Kramer, L. L. Cook, R. S. Fulton, D. L. Johnson, P. J. Minx, S. W. Clifton, T. Hawkins, E. Branscomb, P. Predki, P. Richardson, S. Wenning, T. Slezak, N. Doggett, J. F. Cheng, A. Olsen, S. Lucas, C. Elkin, E. C. Uberbacher, M. Frazier, R. A. Gibbs, D. M. Muzny, S. E. Scherer, J. B. Bouck, E. J. Sodergren, K. C. Worley, C. M. Rives, J. H. Gorrell, M. L. Metzker, S. L.

16

Naylor, R. S. Kucherlapati, D. L. Nelson, G. M. Weinstock, Y. Sakaki, A. Fujiyama, M. Hattori, T. Yada, A. Toyoda, T. Itoh, C. Kawagoe, H. Watanabe, Y. Totoki, T. Taylor, J. Weissenbach, R. Heilig, W. Saurin, F. Artiguenave, P. Brottier, T. Bruls, E. Pelletier, C. Robert, P. Wincker, A. Rosenthal, M. Platzer, G. Nyakatura, S. Taudien, A. Rump, H. M. Yang, J. Yu, J. Wang, G. Y. Huang, J. Gu, L. Hood, L. Rowen, A. Madan, S. Z. Qin, R. W. Davis, N. A. Federspiel, A. P. Abola, M. J. Proctor, R. M. Myers, J. Schmutz, M. Dickson, J. Grimwood, D. R. Cox, M. V. Olson, R. Kaul, C. Raymond, N. Shimizu, K. Kawasaki, S. Minoshima, G. A. Evans, M. Athanasiou, R. Schultz, B. A. Roe, F. Chen, H. Q. Pan, J. Ramser, H. Lehrach, R. Reinhardt, W. R. McCombie, M. de la Bastide, N. Dedhia, H. Blocker, K. Hornischer, G. Nordsiek, R. Agarwala, L. Aravind, J. A. Bailey, A. Bateman, S. Batzoglou, E. Birney, P. Bork, D. G. Brown, C. B. Burge, L. Cerutti, H. C. Chen, D. Church, M. Clamp, R. R. Copley, T. Doerks, S. R. Eddy, E. E. Eichler, T. S. Furey, J. Galagan, J., Gilbert, C. Harmon, Y. Hayashizaki, D. Haussler, H. Hermjakob, K. Hokamp, W. H. Jang, L. S. Johnson, T. A. Jones, S. Kasif, A. Kaspryzk, S. Kennedy, W. J. Kent, P. Kitts, E. V. Koonin, I. Korf, D. Kulp, D. Lancet, T. M. Lowe, A. McLysaght, T. Mikkelsen, J. V. Moran, N. Mulder, V. J. Pollara, C. P. Ponting, G. Schuler, J. R. Schultz, G. Slater, A. F. A. Smit, E. Stupka, J. Szustakowki, D. Thierry-Mieg, J. Thierry-Mieg, L. Wagner, J. Wallis, R. Wheeler, A. Williams, Y. I. Wolf, K. H. Wolfe, S. P. Yang, R. F. Yeh, F. Collins, M. S. Guyer, J. Peterson, A. Felsenfeld, K. A. Wetterstrand, A. Patrinos, M. J. Morgan, P. de Jong, J. J. Catanese, K. Osoegawa, H. Shizuya, S. Choi, Y. J. Chen, J. Szustakowki, International Human Genome Sequencing Consortium, *Nature* 2001, 409, 860-921.

[39] L. R. Bollu, A. Mazumdar, M. I. Savage, P. H. Brown, *Clin. Cancer Res.* **2017**, 23, 2136-2142.

[40] B. G. Neel, N. K. Tonks, *Curr. Opin. Cell. Biol.* **1997**, 9, 193-204.

[41] S. Galic, C. Hauser, B. B. Kahn, F. G. Haj, B. G. Neel, N. K. Tonks, T. Tiganis, *Mol. Cell. Biol.* **2005**, 25, 819-829.

[42] J. Boucher, A. Kleinridders, C. R. Kahn, *Cold Spring Harb. Perspect. Biol.* **2014**, 6, a009191.

[43] E. Swiderska, J. Strycharz, A. Wróblewski, J. Szemraj, J. Drzewoski, A. Sliwinska, *IntechOpen,* **2018**. Available from: https://www.intechopen.com/online-first/role-of-pi3k-akt-pathway-in-insulin-mediated-glucose-uptake.

[44] S. C. Yip, S. Saha, J. Chernoff, *Trends Biochem. Sci.* **2010**, 35, 442-449.

[45] M. Elchebly, P. Payette, E. Michaliszyn, W. Cromlish, S. Collins, A. L. Loy, D. Normandin, A. Cheng, J. Himms-Hagen, C. C. Chan, C. Ramachandran, M. J. Gresser, M. L. Tremblay, B. P. Kennedy, *Science* **1999**, 283, 1544-1548.

[46] L. D. Klaman, O. Boss, O. D. Peroni, J. K. Kim, J. L. Martino, J. M. Zabolotny, N. Moghal, M. Lubkin, Y. B. Kim, A. H. Sharpe, A. Stricker-Krongrad, G. I. Shulman, B. G. Neel, B. B. Kahn, *Mol. Cell. Biol.* **2000**, 20, 5479-5489.

[47] B. P. Kennedy, C. Ramachandran, *Biochem. Pharmacol.* **2000**, 60, 877-883.

[48] C. Ramachandran, B. P. Kennedy, *Curr. Top. Med. Chem.* **2003**, 3, 749-757.

[49] E. Panzhinskiy, J. Ren, S. Nair, *PLoS ONE* **2013**, 8, e77228.

[50] S. S. Abdelsalam, H. M. Korashy, A. Zeidan, A. Agouni, *Biomolecules* **2019**, 9, 286.

[51] O. Ukkola, M. Santaniemi, *J. Intern. Med.* **2002**, 251, 467-475.

[52] N. Krishnan, C. A. Bonham, I. A. Rus, O. K. Shrestha, C. M. Gauss, A. Haque, A. Tocilj, L. Joshua-Tor, N. K. Tonks, *Nat. Commun.* **2018**, 9, 283.

[53] N. Krishnan, K. F. Konidaris, G. Gasser, N. K. Tonks, *J. Biol. Chem.* **2018**, 293, 1517-1525.

[54] M. Sarmiento, Y. A. Puius, S. W. Vetter, Y. F. Keng, L. Wu, Y. Zhao, D. S. Lawrence, S. C. Almo, Z. Y. Zhang, *Biochemistry* **2000**, 39, 8171-8179.

[55] J. P. Sun, A. A. Fedorov, S. Y. Lee, X. L. Guo, K. Shen, D. S. Lawrence, S. C. Almo, Z. Y. Zhang, *J. Biolog. Chem.* **2003**, 278, 12406-12414.

[56] V. V. Vintonyak, A. P. Antonchick, D. Rauh, H. Waldmann, *Curr. Opin. Chem. Biol.* **2009**, 13, 272-283.

[57] H. S. Andersen, O. H. Olsen, L. F. Iversen, A. L. P. Sorensen, S. B. Mortensen, M. S. Christensen, S. Branner, T. K. Hansen, J. F. Lau, L. Jeppesen, E. J. Moran, J. Su, F. Bakir, L. Judge, M. Shahbaz, T. Collins, T. Vo, M. J. Newman, W. C. Ripka, N. P. H. Moller, *J. Med. Chem.* **2002**, 45, 4443-4459.

[58] G. Liu, *Curr. Med. Chem.* **2003**, 10, 1407-1421.

[59] C. Dufresne, P. Roy, Z. Wang, E. Asante-Appiah, W. Cromlish, Y. Boie, F. Forghani, S. Desmarais, Q. Wang, K. Skorey, D. Waddleton, C. Ramachandran, B. P. Kennedy, L. Xu, R. Gordon, C. C. Chan, Y. Leblanc, *Bioorg. Med. Chem. Lett.* **2004**, 14, 1039-1042.

[60] B. Douty, B. Wayland, P. J. Ala, M. J. Bower, J. Pruitt, L. Bostrom, M. Wei, R. Klabe, L. Gonneville, R. Wynn, T. C. Burn, P. C. Liu, A. P. Combs, E. W. Yue, *Bioorg. Med. Chem. Lett.* **2008**, 18, 66-71.

[61] R. B. Sparks, P. Polam, W. Zhu, M. L. Crawley, A. Takvorian, E. McLaughlin, M. Wei, P. J. Ala, L. Gonneville, N. Taylor, Y. Li, R. Wynn, T. C. Burn, P. C. Liu, A. P. Combs, *Bioorg. Med. Chem. Lett.* **2007**, 17, 736-740.

[62] B. R. Bhattarai, B. Kafle, J. S. Hwang, D. Khadka, S. M. Lee, J. S. Kang, S. W. Ham, I. O. Han, H. Park, H. Cho, *Bioorg. Med. Chem. Lett.* **2009**, 19, 6161-6165.

[63] B. R. Bhattarai, B. Kafle, J. S. Hwang, S. W. Ham, K. H. Lee, H. Park, I. O. Han, H. Cho, *Bioorg. Med. Chem. Lett.* **2010**, 20, 6758-6763.

[64] M. Stuible, L. Zhao, I. Aubry, D. Schmidt-Arras, F. D. Bohmer, C. J. Li, M. L. Tremblay, *ChemBioChem* **2007**, 8, 179-186.

[65] https://clinicaltrials.gov

[66] Y. Tang, X. Zhang, Z. Chen, W. Yin, G. Nan, J. Tian, F. Ye, Z. Xiao, *Acta Pharm. Sin. B.* **2018**, 8, 919-932.

[67] J. Sun, C. Qu, Y. Wang, H. Huang, M. Zhang, H. Li, Y. Zhang, Y. Wang, W. Zou, *Mol. Biol.* **2016**, 5, 174-179.

[68] S. Petry, K. H. Baringhaus, S. Hoelder, G. Mueller, US Patent US7211592B2, **2007**.

[69] G. -B. Liang, X. Liao, W. Liu, P. E. Finke, D. Kim, L. Yang, S. Lin, US Patent US8399507B2, **2013**.

[70] S. Gupta, G. Pandey, N. Rahuja, A. K. Srivastava, A. K. Saxena, *Bioorg. Med. Chem. Lett.* **2010**, 20, 5732-5734.

[71] S. Hidalgo-Figueroa, S. Estrada-Soto, J. J. Ramirez-Espinosa, P. Paoli, G. Lori, I. Leon-Rivera, G. Navarrete-Vazquez, *Biomed. Pharmacother.* **2018**, 107, 1302-1310.

[72] M. K. Mahapatra, R. Kumar, M. Kumar, *Med. Chem. Res.* **2017**, 26, 1176-1183.

[73] Z. Wang, Z. Liu, W. Lee, S. N. Kim, G. Yoon, S. H. Cheon, *Bioorg. Med. Chem. Lett.* **2014**, 24, 3337-3340.

[74] S. K. Verma, T. Rajpoot, M. K. Gautam, A. K. Jain, S. Thareja, *Lett. Drug Des. Discov.* **2016**, 13, 295-300.

17

[75]   N. G. Aher, B. Kafle, H. Cho, *Bull. Korean Chem. Soc.* **2013**, 34, 1275-1277.

[76]   K. Varshney, A. K. Gupta, A. Rawat, R. Srivastava, A. Mishra, M. Saxena, A. K. Srivastava, S. Jain, A. K. Saxena, *Chem. Biol. Drug Des.* **2019**, 94, 1378-1389.

[77]   C. A. Ganou, P. T. Eleftheriou, P. Theodosis-Nobelos, M. Fesatidou, A. A. Geronikaki, T. Lialiaris, E. A. Rekka, *SAR QSAR Environ. Res.* **2018**, 29, 133-149.

[78]   K. Varshney, S. Gupta, N. Rahuja, A. K. Rawat, N. Singh, A. K. Tamarkar, A. K. Srivastava, A. K. Saxena, *ChemMedChem* **2012**, 7, 1185-1190.

[79]   S. Gupta, K. Varshney, R. Srivastava, N. Rahuja, A. K. Rawat, A. K. Srivastava, A. K. Saxena, *Med. Chem. Commun.* **2013**, 4, 1382-1387.

[80]   J. N. Andersen, N. K. Tonks, *Top. Curr. Genet.* **2004**, 5, 201-230.

[81]   J. Montalibet, B. P. Kennedy, *Drug Discovery Today: Ther. Strateg.* **2005**, 2, 129-135.

[82]   D. P. Wilson, Z. K. Wan, W. X. Xu, S. J. Kirincich, B. C. Follows, D. Joseph-McCarthy, K. Foreman, A. Moretto, J. Wu, M. Zhu, E. Binnun, Y. L. Zhang, M. Tam, D. V. Erbe, J. Tobin, X. Xu, L. Leung, A. Shilling, S. Y. Tam, T. S. Mansour, J. Lee, *J. Med. Chem.* **2007**, 50, 4681-4698.

[83]   M. V. Reddy, C. Ghadiyaram, S. K. Panigrahi, N. R. Krishnamurthy, S. Hosahalli, A. P. Chandrasekharappa, D. Manna, S. E. Badiger, P. K. Dubey, L. N. Mangamoori, *Protein Pept. Lett.* **2014**, 21, 90-93.

[84]   A. D. Patel, R. Barot, I. Parmar, I. Panchal, U. Shah, M. Patel, B. Mishtry, *Curr. Comput. Aided Drug Des.* **2018**, 14, 349-362.

[85]   G. Pandey, A. K. Saxena, *J. Chem. Inf. Model.* **2006**, 46, 2579-2590.

[86]   V. M. Balaramnavar, R. Srivastava, N. Rahuja, S. Gupta, A. K. Rawat, S. Varshney, H. Chandasana, Y. S. Chhonker, P. K. Doharey, S. Kumar, S. Gautam, S. P. Srivastava, R. S. Bhatta, J. K. Saxena, A. N. Gaikwad, A. K. Srivastava, A. K. Saxena, *Eur. J. Med. Chem.* **2014**, 87, 578-594.

[87]   D. Seeliger, B. L. de Groot, *J. Comput. Aided Mol. Des.* **2010**, 24, 417-422.

[88]   D. S. Goodsell, G. M. Morris, A. J. Olson, *J. Mol. Recognition.* **1996**, **9,** 1-5.

[89]   D. E. V. Pires, T. L. Blundell, D. B. Ascher, *J. Med. Chem.* **2015**, 58, 4066-4072.

[90]   M. N. Drwal, P. Banerjee, M. Dunkel, M. R. Wettig, R. Preissner, *Nucleic Acids Res.* **2014**, 42, Web Server issue, W53-W58.

[91]   P, Banerjee, A. O. Eckert, A. K. Schrey, R.Preissner, *Nucleic Acids Res.* **2018**, 46, Web Server issue, W257-W263.

[92]   G. Revelant, S. Huber-Villaume, S. Dunand, G. Kirsch, H. Schohn, S. Hesse, *Eur. J. Med. Chem.* **2015**, 94, 102-112.

[93]   I. Apostolidis, K. Liaras, A. Geronikaki, D. Hadjipavlou-Litina, A. Gavalas, M. Sokovic, J. Glamoclija, A. Ciric, *Bioorg. Med. Chem.* **2013**, 21, 532-539.

[94]   Calbiochem PTP1B Assay Kit, Colorimetric, User Protocol. **2008**, Catalogue No: 539736.

[95]   R. K. P. Tripathi, O. Goshain, S. R. Ayyannan, *ChemMedChem.* **2013**, 8, 462-474.

18

## Entry for the Table of Contents



A library of 15 thiazolidin-4-one derivatives was designed, synthesized and evaluated for *in-vitro* PTP1B inhibitory activity. The compounds proved to be potent PTP1B inhibitors with $IC_{50}$ in micromolar range. Compound **17** (shown) emerged as lead PTP1B inhibitor both experimentally ($IC_{50}$=5.88±0.06 µM, $K_i$=16.98±2.69 µM) and computationally (ΔG=-8.05 kcal mol$^{-1}$; $K_i$=1.26 µM).